Tsunami history of an Oregon coastal lake reveals a 4600 yr record of great earthquakes on the Cascadia subduction zone

Harvey M. Kelsey†
Department of Geology, Humboldt State University, Arcata, California 95521, USA

Alan R. Nelson
U.S. Geological Survey, M.S. 966, P.O. Box 25046, Denver, Colorado 80225-0046, USA

Eileen Hemphill-Haley
Department of Geology, Humboldt State University, Arcata, California 95521, USA

Robert C. Witter
William Lettis and Assoc., Inc., Suite 262, 1777 Botelho Drive, Walnut Creek, California 94596, USA

ABSTRACT

Bradley Lake, on the southern Oregon coastal plain, records local tsunamis and seismic shaking on the Cascadia subduction zone over the last 7000 yr. Thirteen marine incursions delivered landward-thinning sheets of sand to the lake from nearshore, beach, and dune environments to the west. Following each incursion, a slug of marine water near the bottom of the freshwater lake instigated a few-year-to-several-decade period of a brackish (≤4‰ salinity) lake. Four additional disturbances without marine incursions destabilized sideslopes and bottom sediment, producing a suspension deposit that blanketed the lake bottom.

Considering the magnitude and duration of the disturbances necessary to produce Bradley Lake's marine incursions, a local tsunami generated by a great earthquake on the Cascadia subduction zone is the only accountable mechanism. Extreme ocean levels must have been at least 5–8 m above sea level, and the cumulative duration of each marine incursion must have been at least 10 min. Disturbances without marine incursions require seismic shaking as well.

Over the 4600 yr period when Bradley Lake was an optimum tsunami recorder, tsunamis from Cascadia plate-boundary earthquakes came in clusters. Between 4600 and 2800 cal yr B.P., tsunamis occurred at the average frequency of ~3–4 every 1000 yr. Then, starting ~2800 cal yr B.P., there was a 930–1260 yr interval with no tsunamis. That gap was followed by a ~1000 yr period with 4 tsunamis. In the last millennium, a 670–750 yr gap preceded the A.D. 1700 earthquake and tsunami. The A.D. 1700 earthquake may be the first of a new cluster of plate-boundary earthquakes and accompanying tsunamis.

Local tsunamis entered Bradley Lake an average of every 390 yr, whereas the portion of the Cascadia plate boundary that underlies Bradley Lake ruptured in a great earthquake less frequently, about once every 500 yr. Therefore, the entire length of the subduction zone does not rupture in every earthquake, and Bradley Lake has recorded earthquakes caused by rupture along the entire length of the Cascadia plate boundary as well as earthquakes caused by rupture of shorter segments of the boundary. The tsunami record from Bradley Lake indicates that at times, most recently ~1700 yr B.P., overlapping or adjoining segments of the Cascadia plate boundary ruptured within decades of each other.

Keywords: tsunami, Cascadia subduction zone, paleoseismology, plate boundaries, subduction zone.

INTRODUCTION

Since the initial discoveries of evidence for regional coastal subsidence during great (>M_w 8) subduction zone earthquakes almost two decades ago (Atwater, 1987; Darienzo and Peterson, 1990), many studies (cited below) have documented repeated plate-boundary earthquakes on the Cascadia subduction zone (Fig. 1). Although the time between Cascadia subduction zone earthquakes varies from as short as a century to as long as 1200 yr, the average recurrence interval of Cascadia subduction zone earthquakes is ~500 yr for those sites with upwards of 3500 yr of earthquake record (Atwater and Hemphill-Haley, 1997; Kelsey et al., 2002; Witter et al., 2003). An offshore record of seismically triggered turbidites at the heads of Cascadia submarine canyons suggests that great earthquakes recur at intervals of ~600 yr, with 13 in the last 7700 yr (Adams, 1990; Goldfinger et al., 2003).

The best documented of the Cascadia subduction zone earthquakes is the most recent one, which occurred on January 26, 1700 (Satake et al., 1996; Jacoby et al., 1997; Yamaguchi et al., 1997). This earthquake was probably a M_w 9, based on the size of the associated tsunami on the Japanese coast as documented in written records (Satake et al., 1996, 2003). An earthquake of such magnitude probably ruptured the entire ~1200 km length of the subduction zone. Tsunami deposits from the A.D. 1700 earthquake are found along the length of the subduction zone from northern California to British Columbia (Garrison-Laney, 1998; Kelsey et al., 1998; Clague and Bobrowsky, 1994; Clague et al., 2000).

Coastal archives of older Cascadia plate-boundary earthquakes are less extensive than those of the A.D. 1700 earthquake, and tsunamis accompanying the older earthquakes go unrecorded in written history. Records of pre–A.D. 1700 great earthquakes come from estuaries in northern California, Oregon, Washington, and British Columbia (Darienzo and Peterson, 1990; Clague, 1996; Nelson et al., 1996; Atwater and

†E-mail: hmk1@humboldt.edu.

GSA Bulletin; July/August 2005; v. 117; no. 7/8; p. 1009–1032; doi: 10.1130/B25452.1; 16 figures; 6 tables; Data Repository item 2005105.

Hemphill-Haley, 1997; Kelsey et al., 2002; Witter et al., 2003) and the continental shelf and slope (Goldfinger et al., 2003). Although uncertainties in ^{14}C dating most great earthquakes are commonly hundreds of years, age correlation of earthquakes among some thoroughly studied sites led Kelsey et al. (2002) and Witter et al. (2003) to conclude that some great earthquakes rupture only part of the plate boundary and so are $<M_w$ 9. This conclusion is consistent with the analysis of segmented structural basins by Wells et al. (2003) at Cascadia.

In this paper we describe another earthquake record for Cascadia, a record of great-earthquake tsunamis preserved in the deposits of Bradley Lake, a low-lying lake on the southern Oregon coast (Fig. 1). Lake-derived tsunami histories on the Cascadia subduction zone and in Scandinavia are discussed by Bondevik et al. (1997), Abramson (1998), Garrison-Laney (1998), and Hutchinson et al. (1997, 2000), although these histories are shorter than the one described here. The coastal lake tsunami record in Bradley Lake is different from paleoseismic records from coastal marshes in that Bradley Lake can record Cascadia tsunamis triggered both by earthquakes that caused the lake coastline to subside and by earthquakes that ruptured only a more northerly (or southerly) section of the subduction zone. The Bradley Lake tsunami record also differs from Cascadia offshore turbidite records in that the lake records tsunamis spaced a few decades apart.

The temporal resolution of the Bradley Lake tsunami record helps document differences in the size and frequency of Cascadia plate-boundary earthquakes not apparent in other Cascadia records. The number of tsunamis recorded in Bradley Lake deposits is greater than the number of earthquakes recorded in directly adjacent coastal marshes. From this we infer that tsunamis unrepresented in the coastal marsh record of great earthquakes near Bradley Lake were generated during earthquakes that ruptured a neighboring portion of the plate boundary. The Bradley Lake tsunami record also shows that, at least for the past 4600 yr, plate-boundary earthquakes occurred in clusters, with interseimic intervals of variable length.

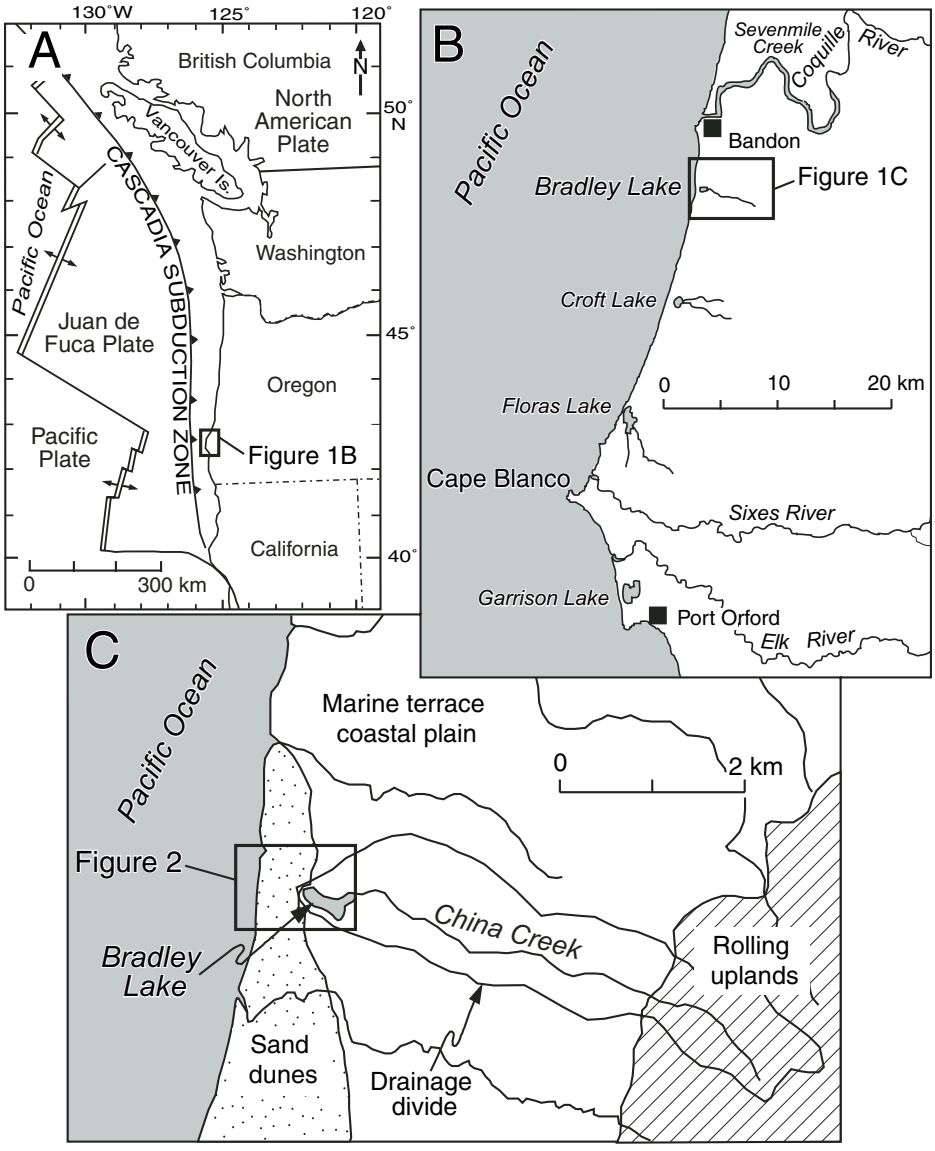

Figure 1. (A) Location of Bradley Lake within the context of the Cascadia subduction zone. (B) Coastal lakes of the southern Oregon coastal plain. (C) China Creek drainage basin and extent of marine terraced landscape east of Bradley Lake.

RESEARCH APPROACH

Bradley Lake's effectiveness as a tsunami recorder is a result of its favorable coastal setting and morphology (Figs. 1 and 2) and the unusually long-lived balance among lake level, sea-level rise, and land uplift along this part of the Oregon coast. As we explain below, Bradley Lake is and has been near an optimal elevation and distance inland to record tsunamis from Cascadia subduction zone earthquakes but probably is too high and too far inland to contain a record of storm waves or tsunamis from distant sources. Of equal importance, Bradley Lake is unusually deep for a coastal lake (10 m); its anoxic bottom water preserves a largely laminated record of lake sediment in which deposits from events that have episodically disturbed the lake sequence are easily preserved and identified. Reconnaissance coring in four coastal lakes of southern Oregon (Fig. 1B) showed that Bradley Lake was the deepest lake and contained the longest lake record, spanning many thousands of years.

A record of repeated marine incursion into Bradley Lake consists of two primary lines of evidence: distinctive associations of lake sediment lithofacies (groupings of vertically adjacent beds) that differ from the freshwater lake sediment deposited by annual lake processes, and diatom assemblages that show lake inundation by marine water. Erosion of underlying freshwater lake sediment during emplacement of the distinctive lithofacies associations suggests repeated lake-wide disturbance events. Evidence for marine inundation during disturbance events is particularly strong when these lithofacies associations contain marine diatoms.

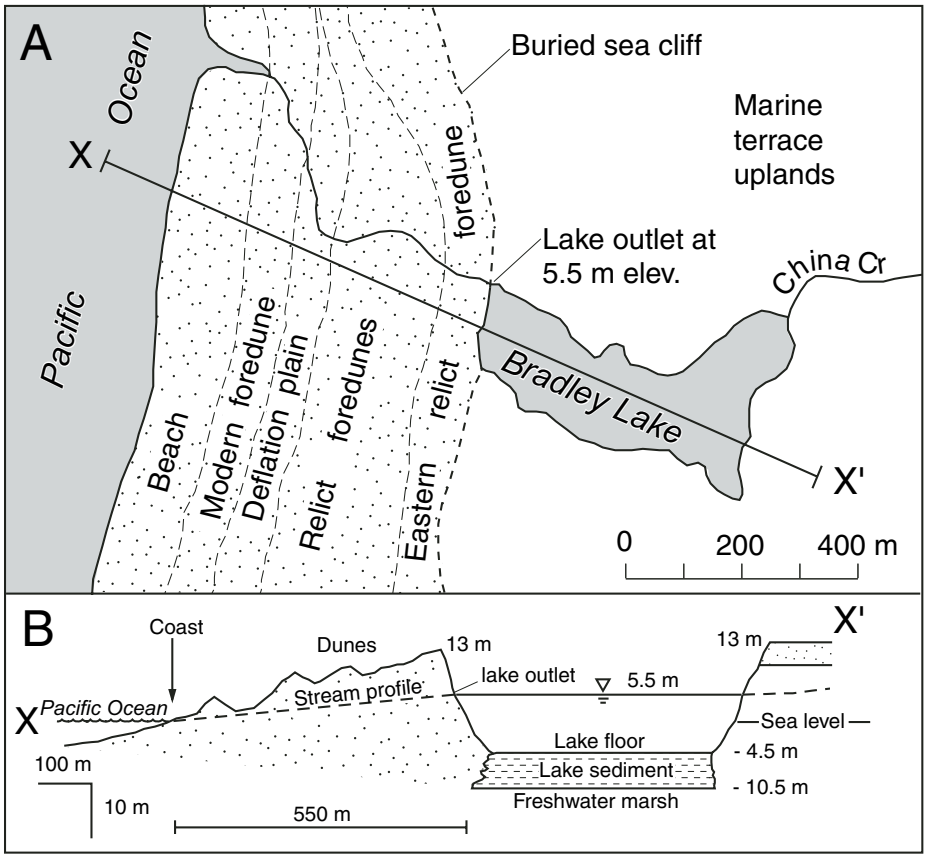

Figure 2. (A) Map of Bradley Lake and coastal dune field between Bradley Lake and Pacific Ocean. (B) Longitudinal topographic cross section from coastline ESE across Bradley Lake to marine terrace upland.

To learn how the lake physically and chemically responded to marine inundation, we described the lithology and stratigraphy of lithofacies associations, tabulated diatom assemblages in the lake sediment, surveyed lake bathymetry, measured seasonal temperature and salinity changes in the lake, and computed a water balance for the lake. To determine if marine inundations were caused by local tsunamis, distant tsunamis, or storm waves, we attempted to reconstruct the elevation history of the lake outlet using relative sea-level data, surveys of the modern lake outlet, and the age and degree of preservation of laminated lake sediment.

METHODS

Bradley Lake stratigraphy was explored with 14 piston cores (50 mm diameter) and 13 vibracores (70 mm diameter) distributed throughout the lake (Fig. 3). Livingston piston cores (Wright, 1967) provided uncompacted sediment intervals but were ineffective in penetrating sand. Through vibracoring (modification of the system of Smith, 1987) we penetrated multiple sand beds as thick as 1.5 m, although the upper 1 m intervals of vibracores were severely compacted. Other field investigations included sounding of the lake using an echo sounder, temperature and salinity measurement throughout the lake column over the course of 2 yr (1996–1997), and surveys of the lake outlet.

Cores were split, described, photographed, sampled, and stored in the core facility at Oregon State University. Laboratory analyses included particle-size distribution measured with X-rays using a Micromeritics 5100 Sedigraph (Fig. DR1[1]), percent organic carbon (Aspila et al., 1976), scanning electron microscopy, and diatom analysis. Diatom samples were collected at selected intervals (193 samples) in order to determine diatom associations in the different sediment types. Diatom sample preparation techniques are discussed in Hemphill-Haley and Lewis (2003). Smear slides of core sediment (186 slides) were analyzed semiquantitatively (e.g., Birks, 1981) using additional microfossil and plant fragment categories after Boulter (1994). Below we describe sample selection and analysis of 61 accelerator mass spectrometry (AMS) ^{14}C ages from the cores and evaluation of the stratigraphic consistency of ages using the statistical program OxCal (Bronk Ramsey, 1995, 2001).

[1]GSA Data Repository item 2005105, Figs. DR1 and DR2: additional data on sediment thickness and sediment textures; Tables DR1 and DR2: tabulate additional data on radiocarbon ages and sedimentation rates, is available on the Web at http://www.geosociety.org/pubs/ft2005.htm. Requests may also be sent to editing@geosociety.org.

BRADLEY LAKE

Bradley Lake is one of a series of southern Oregon coastal lakes impounded behind Holocene dunes (Figs. 1 and 2). The lake formed because China Creek, which incised a 24-m-deep canyon into a marine terrace surface (Fig. 2), was blocked at the canyon mouth by a beach foredune that built up as the coast stabilized during the mid-Holocene deceleration in rate of eustatic sea-level rise (Stanley and Warne, 1994). The floor of the lake is ~4.0–5.0 m below sea level because the lake's outlet is at 5.5 m elevation (NGVD, National Geodetic Vertical Datum of 1929), and the lake is 9.5–10.5 m deep (Figs. 2 and 3).

Our coring reveals that the lake is underlain by 6 m of lacustrine sediment (Fig. 4) and that in three cores where we penetrated through the 6 m of lake sediment, the first meter of strata below the lake sediment consists of freshwater marsh peat (cores E, X, and F, Fig. 4).

Radiocarbon ages (discussed extensively below) indicate that Bradley Lake formed 7300 yr ago on the site of a freshwater marsh. Diatom observations throughout the lake section (also discussed extensively below) show that the lake has been fresh throughout its lifespan but that marine diatoms were transported into the lake during disturbance events.

Bradley Lake surface temperatures fluctuate from ~8 °C to 23 °C whereas bottom temperatures in the lake are ~7 °C to 9 °C throughout the year (Fig. 5). Isothermal conditions (same temperature throughout its depth), which are more favorable to lake mixing, characterize the lake from approximately mid-December to mid-March (Fig. 5). Therefore the conditions that optimally would allow chemical diffusion of more saline bottom water up to the surface occur four or fewer months a year. Conversely, during eight or more months of the year there is a well-developed thermocline (plane of greatest thermal gradient) at ~4 m (Fig. 5), and lake inflow and outflow mainly involves water above 4 m depth.

The main source of water to Bradley Lake is streamflow from China Creek (Fig. 1; Table 1). Assuming no net change in water surface elevation over the course of a year, annual loss of water from Bradley Lake is the consequence of stream discharge at the outlet (~99% of total input), evaporation from the lake surface (~1% of total input), and minor amounts of groundwater seepage through the sand dune at the west end of the lake (Table 1).

The volume of water that comes into and leaves Bradley Lake each year is ~7.4 times the lake volume (Table 1). Assuming the volume of water above the thermocline is well mixed and readily transported through the lake basin, whereas the volume of water below the thermocline is denser and relatively stagnant for most of the year, then the transportable volume of water in the upper ~4 m of the lake may be replenished close to fifteen times each year.

Seasonal variation in the character and intensity of sedimentation in Bradley Lake causes deposition and preservation of laminated sediment in most years. Although most distinct sediment laminae reflect seasonal differences in sedimentation, as we explain below, laminae thickness and degree of preservation are too inconsistent for the laminae to be (annual) varves in portions of the lake sediment section. Thermal stratification of Bradley Lake and less frequent saline stratification (explained below) partially buffer deep laminated lake sediment from mixing processes (e.g., Larsen and MacDonald, 1993). Organic sediment contributed by diatoms, algae, and vascular plants and clay and silt contributed from runoff and lakeshore wave erosion may be deposited and buried undisturbed, or may be mixed by bioturbation or by currents generated by wind waves or thermal destratification (overturn; e.g., Wetzel, 2001). Less frequent processes with greater potential for mixing deep sediment include slumping of sediment from lake sideslopes and turbidity flows induced by wind waves, large floods on China Creek, or shaking and seiche due to earthquake ground motions. Such events may induce bottom currents strong enough to erode and redeposit sediment over parts, but normally not all, of the lake bottom.

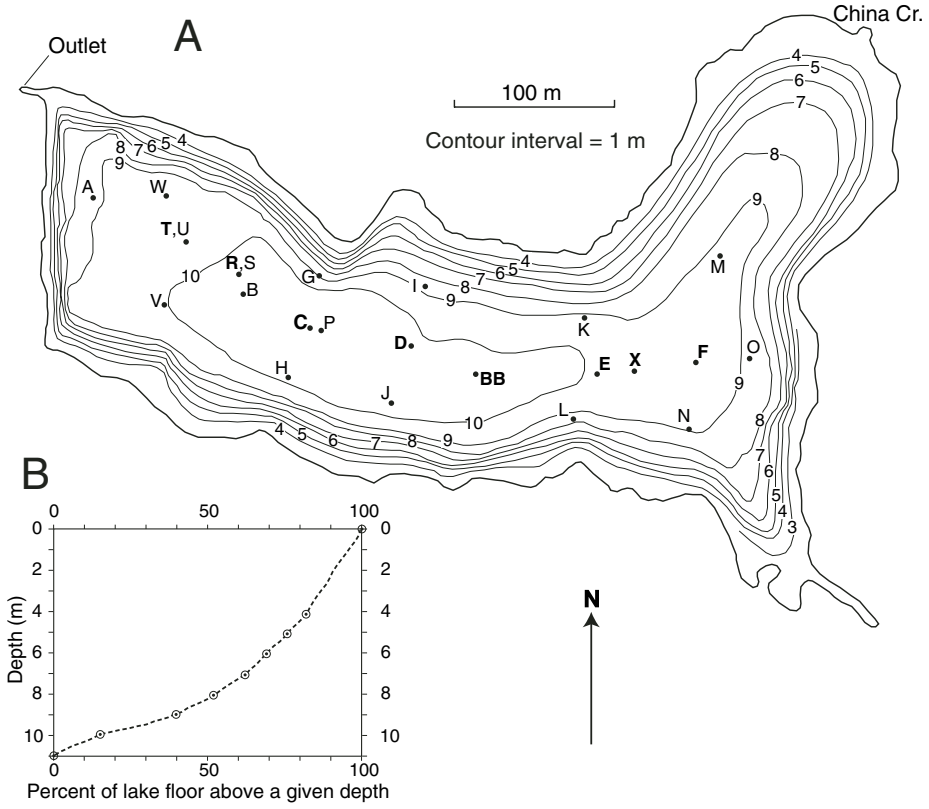

Figure 3. (A) Bathymetry (depth contours in meters) and core site locations for Bradley Lake. Cores denoted by bold letters are depicted in Figure 4. (B) Cumulative frequency profile showing the percent of area of lake floor above a given depth.

SEDIMENTS IN BRADLEY LAKE

A compilation of core stratigraphy along the central lake axis (Figs. 3 and 4) shows that the lake sediment consists of laminated mud interbedded with muddy debris and sand units. We divide the sediment into seven lithofacies using sediment characteristics and into three biofacies based on diatom assemblages (Hemphill-Haley and Lewis, 2003). We use facies characteristics and spatial relations to define two facies associations; the first includes facies that are primarily the result of processes typical of the annual cycle of lake sedimentation and the second includes facies that record episodic events that disturbed the entire lake (disturbance events).

Distinctive lithologies and marker beds make correlation of Bradley Lake cores unusually precise. Lake deposits consist primarily of laminated mud interbedded with thin but distinctive sequences of massive organic-rich mud, sandy mud, and sand. The distinctive spacing, thickness, and sequence of massive organic-rich mud and sandy beds and the distinctive patterns of light and dark laminae between them allow us to confidently correlate cores throughout the lake (Figs. 4, 6, 7, and 8). We identified 82 correlation points on core photographs, 14 of which are common to 17 of the 21 described cores. The four longest axial cores (E, F, X, and BB, Fig. 4) have 44 points in common, including the basal contact of the 17 disturbance event beds.

Laminated Mud Facies

Laminated-mud sequences consist of distinct, continuous couplets of light and dark laminae. In most cases, couplets consist of a light, gray, clay-rich laminae and a dark, black or brown, organic-rich laminae (Figs. 6, 7, and 8). Brown and black laminae are ~0.5–1.0 mm in thickness and, based on smear-slide microscopy, are dominated by decomposed plant fragments (Fig. 7) with common to abundant diatoms. Although there is a compositional continuum between black and brown laminae, black laminae (Munsell color 5Y-2.5Y–10YR 2/2–2/1) tend to consist of finer, highly decomposed organic particles (most <0.1 mm) with common pyrite spheroids and little silt or clay (<30% clay and silt by volume), whereas brown laminae (Munsell color 2.5Y–10YR 2/1–4/2) contain coarser plant fragments (<0.1–1.0 mm) and moderate amounts of clay with a little silt (30%–50% clay and silt). Under a scanning electron microscope, brown laminae are texturally coarser than gray laminae, the texture being a product of abundant, coarse, interlocking, decomposed plant fragments. We infer that black laminae record periods of minimal clastic input with no bottom disturbance, whereas brown laminae may record either times of increased input of detrital organic material or mixing of sediment in previously deposited light and dark laminae.

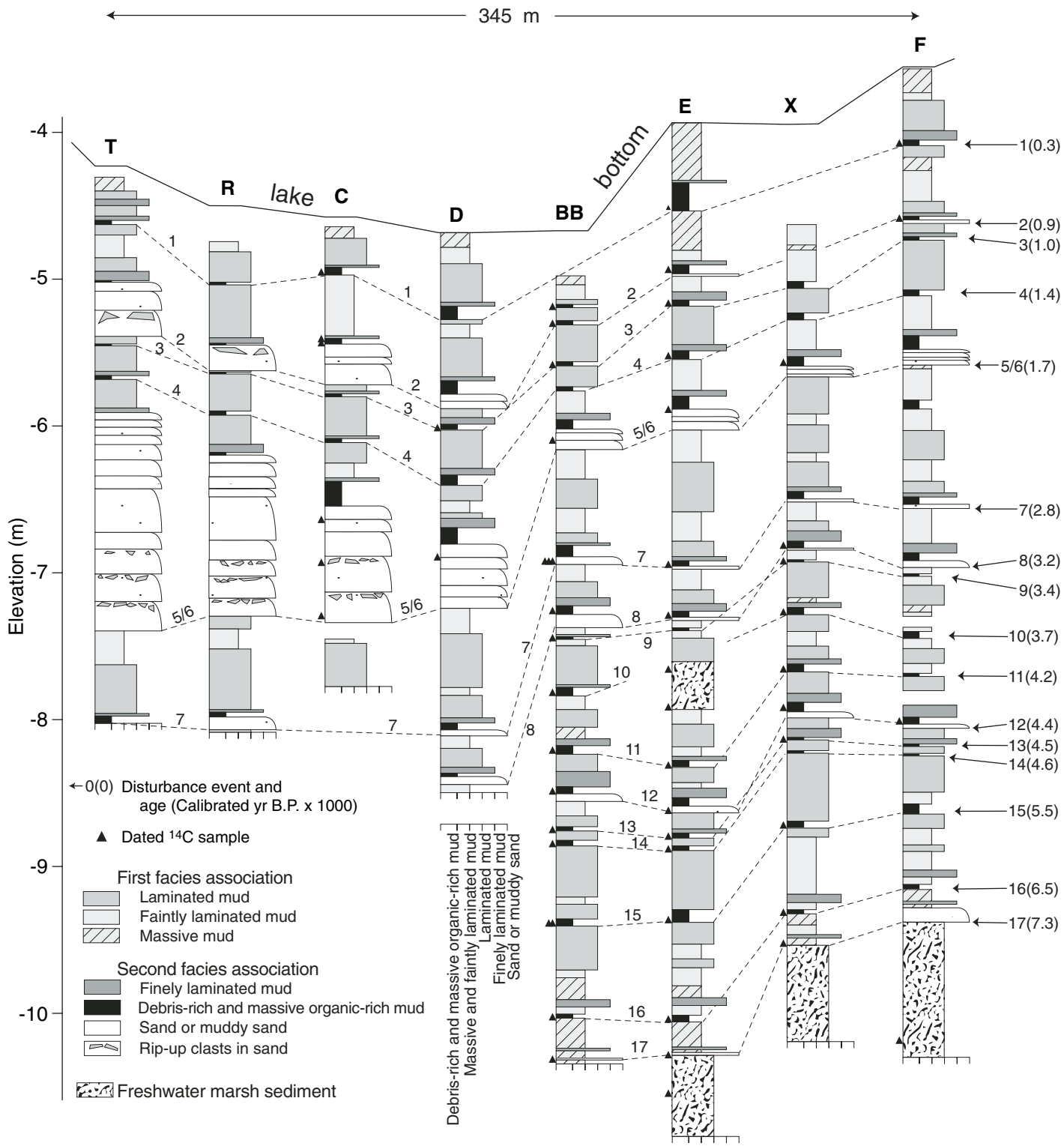

Figure 4. Plot of selected cores taken along central axis of Bradley Lake. 60× vertical exaggeration. Mean horizontal distance between cores is 50 m; actual distance between cores ranges from 20 to 80 m. Cores C, D, E, and F are piston cores; cores T, R, BB, and X are vibracores and show coring-induced sediment compaction in upper ~1.5 m of core. Sand units show individual depositional pulses; the number of pulses reflect the actual number counted in the core. Rip-up clasts occur at top of pulses; however, not all horizons containing rip-up clasts could be shown.

Based on smear-slide microscopy and grain-size analysis (Fig. DR1; see footnote 1), gray laminae (Munsell color 2.5Y–5Y 5/1–6/1) are 60%–80% clay by volume and contain few fine and almost no coarse organic particles (Fig. 7). In most gray laminae, diatoms are rare or absent, but in a few laminae they are common. Gray laminae have a much greater thickness range (0.3–20 mm) than dark laminae, although the modal thickness (0.5–1.5 mm) is similar to that for dark laminae. Some gray laminae are draped over unconformities that truncate underlying laminae. Thick gray laminae (≥1.0 mm) usually occur in 50- to 150-mm-thick well-laminated intervals of the laminated mud facies. Gray laminae record the deposition of clay and silt derived from exposures of Pleistocene or Tertiary sediment near the lake shore or carried into the lake by China Creek (Fig. 2).We infer that intervals with thick gray clay laminae represent periods, spanning up to tens of years, of unusually stormy winters when China Creek delivered much suspended sediment to the lake.

The lake-wide continuity of gray laminae is striking—some can be correlated to the millimeter throughout the lake. Many individual laminae within laminated mud facies can be traced throughout the lake and do not markedly thicken or thin from one part of the lake to another. However, some gray laminae are compositionally gradational with alternating darker laminae, vary widely in thickness, and are discontinuous, truncated, or indistinct in parts of the section (Fig. 8).

Finely Laminated Mud Facies

Finely laminated mud facies contain primarily black and gray laminae that are <0.5 mm thick, continuous, and of uniform thickness (Fig. 8). Finely laminated mud facies occur consistently directly above massive organic-rich mud facies and are in turn gradational upward into overlying laminated mud facies (Figs. 4, 6, and 7). Short intervals of finely laminated mud also occur locally within long intervals of laminated mud facies.

Although the variable composition and thickness of the light and dark laminae of laminated mud facies (Fig. 8A) make them less likely to be (annual) varves, we infer that the more distinct light-dark laminae couplets of the finely laminated mud facies (Fig. 8B) are varves. The uniform thickness and continuity of the couplets throughout the lake sediment section are more typical of varves produced by seasonal changes in sedimentation than by sudden events that strongly affected only part of the lake basin, such as storms or landslides. The slow sedimentation rates implied by the <0.5-mm-thick,

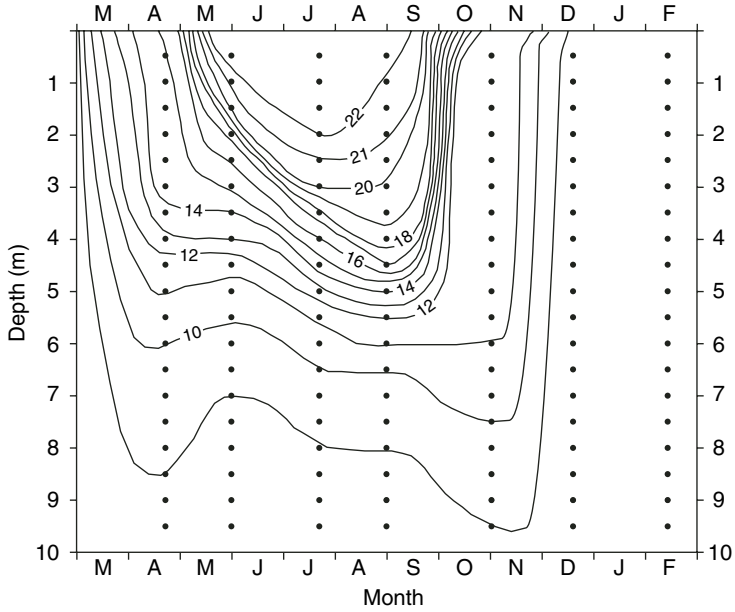

Figure 5. Isothermal variations in Bradley Lake, March 1996 to February 1997. Contours are degrees Celsius, dots are sample depths.

TABLE 1. VOLUME AND WATER BALANCE FOR BRADLEY LAKE

Quantity	Volume of water ($m^3 \times 10^3$)	Equivalent depth (m) over lake surface (lake surface = 92.2×10^3 m^2)
Volume of lake[†]	662.1	7.2
Volume of lake above thermocline at 4 m depth[‡]	335.7	3.6
Annual input		
1. Direct precipitation onto lake[§]	133.0	.44
2. Groundwater seepage into lake from north and south sides[#]	8.18	0.089
3. Stream discharge into lake[††]	4758	51.61
Total annual input	4899	53.14
Annual output		
1. Evaporation from lake[‡‡]	56.2	0.610
2. Groundwater seepage through dune barrier at west end of lake[§§]	2.1	0.002
3. Stream discharge out of lake (calculated by assuming zero change in water storage within lake over the course of one year)	4841	52.50
Total annual output	4899	53.11

[†]Volume of lake computed from bathymetric map with 1 m depth contours (Fig. 3).

[‡]Thermocline is at 4 m depth, determined from temperature-depth profiles taken during the 1996–1997 season.

[§]Annual precipitation is the 30 yr average (1961–1990) for the Bandon 2 NNE precipitation gage (Garwood, 1996) 7.7 km northeast of Bradley Lake at 75 m elevation.

[#]Annual groundwater seepage into Bradley Lake assumes seepage through the north and south walls and bottom of the lake from a sandy siltstone aquifer (hydraulic conductivity = 10^{-6} m/s; hydraulic gradient = 0.015). Contributing aquifer thickness is assumed to be twice the lake depth. Water table slope (hydraulic gradient) is assumed to mimic the topographic slope into the lake from the north and from the south.

[††]Annual stream discharge into lake is the difference between annual precipitation (30 yr average at the Bandon 2 NNE precipitation gage, see above footnote) and actual evapotranspiration (AET). AET is calculated from the 30 yr (1961–1990) monthly temperature averages for Bandon 2 NNE precipitation gage through calculation of a 12-month water balance using procedures outlined in Thornthwaite and Mather (1995) and Dunner and Leopold (1978).

[‡‡]Annual evaporation from the lake is taken from a map of mean annual lake evaporation for the United States for 1946–1955 [Figs. 4–10, p. 118, Dunner and Leopold (1978)].

[§§]Annual groundwater seepage through sand barrier assumes lake water leaks from the west end sand barrier through sand aquifer (aquifer thickness = 5 m; hydraulic conductivity = 10^{-5} m/s) toward the beach along a hydraulic gradient of 0.01 (5 m water table drop over 500 m distance from lake to beach).

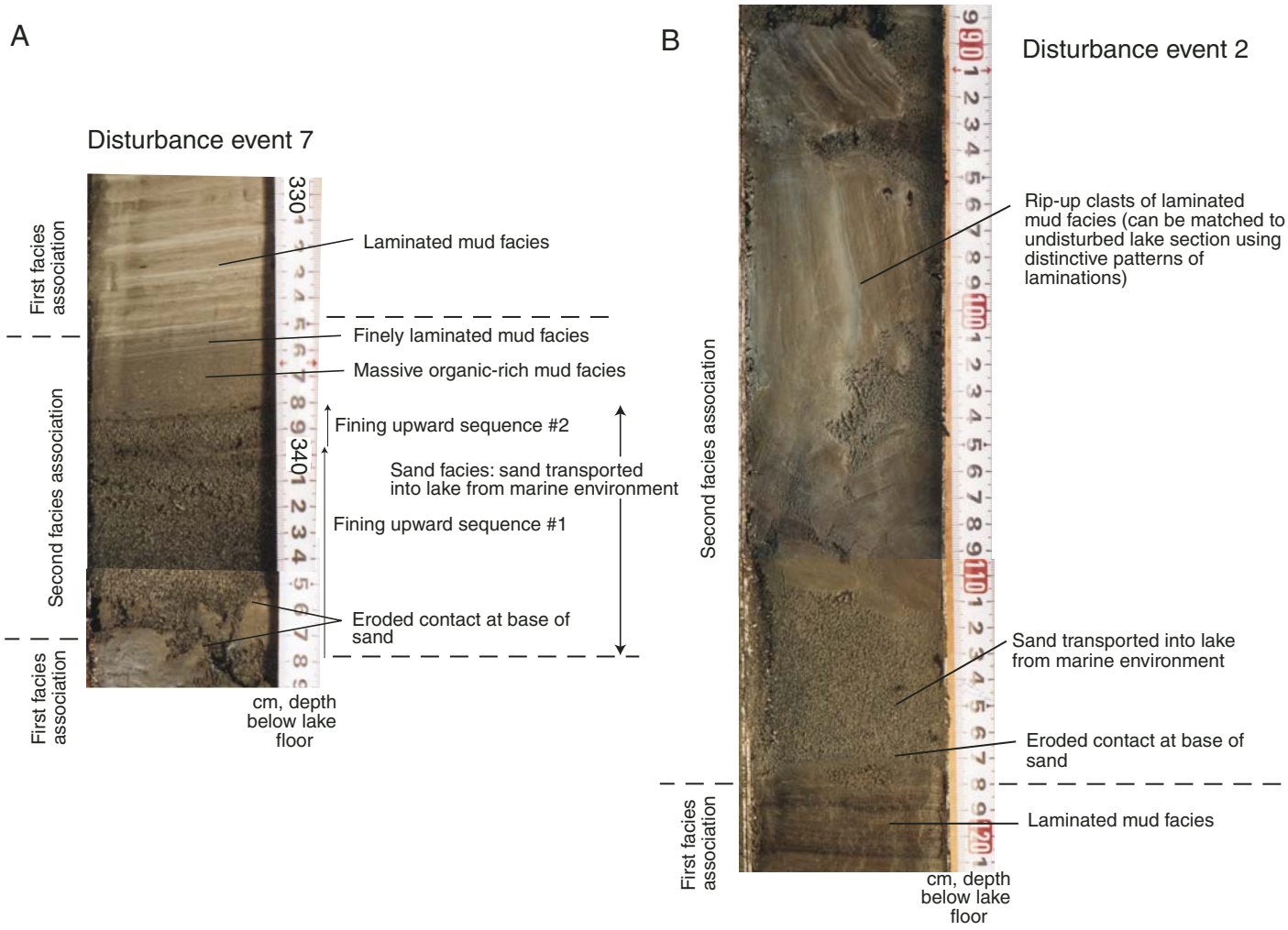

Figure 6. (A) Photograph of disturbance event 7 in core R, showing characteristic sediment facies and facies associations. (B) Photograph of basal pulse of disturbance event 2 sand in core T, showing rip-up clasts of laminated mud facies at top of this pulse.

organic-rich, dark laminae that we infer were deposited in summer suggest that the couplets span at least a year. At such sedimentation rates, pulses of clay carried into the lake by China Creek that were separated by days to months would appear in cores as the single light laminae of a couplet.

Detailed analyses that would demonstrate seasonal associations for the light-dark couplets (e.g., Peglar et al., 1984; Bradbury and Dean, 1993; Dean et al., 1999) are beyond the scope of this study; however, the couplets are lithologically similar to those described from many cool-climate lakes with seasonal clastic input (Page et al., 1994; Hughen, 1996; Anderson, 1996; Larsen et al., 1998; Ojala et al., 2000). For example, in Loe Pool, a coastal freshwater lake in southwest England with a setting similar to that of Bradley Lake, black/dark-brown, diatom-rich laminae deposited in summer alternate with gray-brown, clay-rich laminae that record increased stream inflow in winter (Simola et al., 1981).

Faintly Laminated Mud Facies

The faintly laminated mud facies consist of black, brown, and gray laminae that are less distinct, frequent, and continuous than laminae in the laminated mud facies. Laminae are barely visible in some sections of core as thick as 50 mm, and distinct gray laminae frequently occur in isolation in faintly laminated mud. Brown laminae are much more common in faintly laminated mud at the expense of black laminae. The faintly laminated mud facies make up ~15% of the lake sediment (Fig. 4).

The faintly laminated mud facies probably formed because of greater postdepositional mixing of organic and mineral components of laminae than was the case for the laminated mud facies. Alternatively, this facies may have formed during years when there was less of a contrast in the intensity of seasonal processes that produce laminae.

Massive Mud Facies

The massive mud facies are brown, contain ~5% <0.1 mm plant fragments, and the mineral component (95%) is 30%–50% silt with the rest being clay (Fig. 7). Massive mud is most common in the lower 0.6 m of the longest lake cores below disturbance event 15 (Fig. 4). Below disturbance event 15, the massive mud has remnants of single laminae suggesting that bioturbation thoroughly mixed previously laminated sediment. In contrast, the massive mud facies above disturbance event 15 does not correlate well among cores, suggesting that it may result

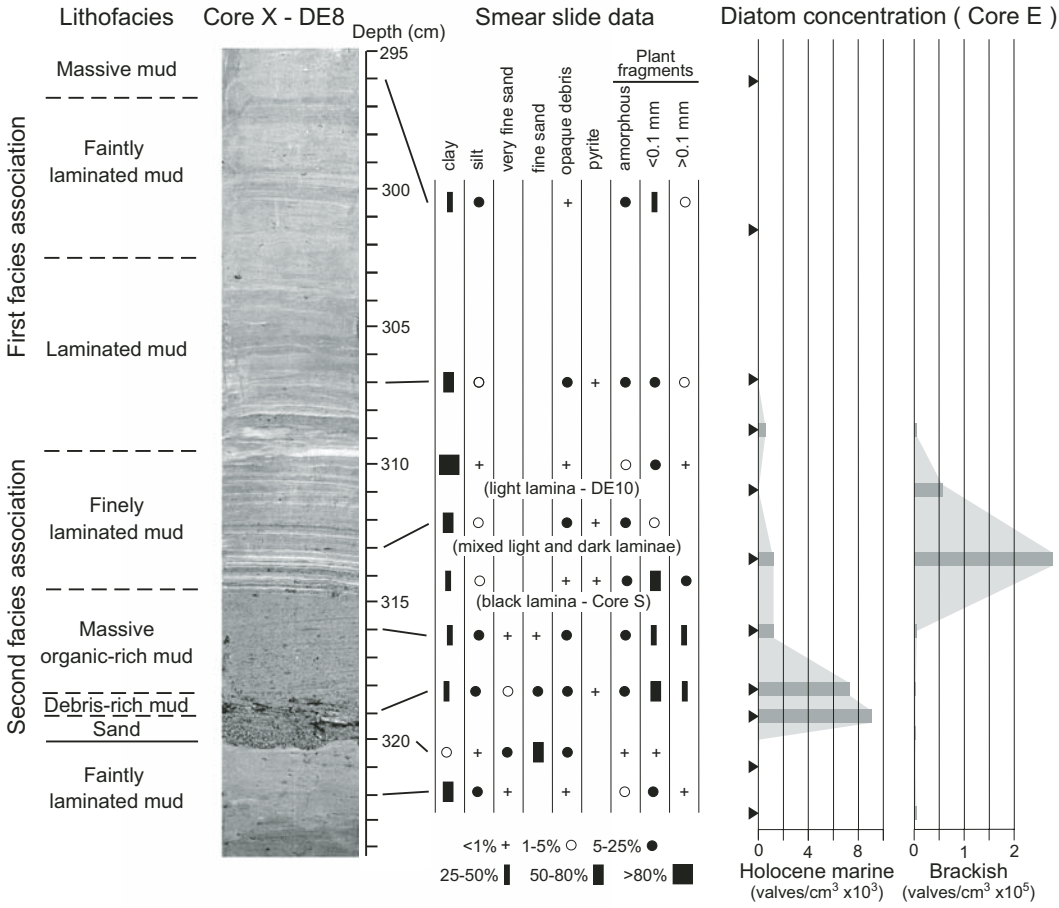

Figure 7. Lithofacies, smear-slide data, and diatom data adjacent to photograph of DE 8 in Core X. Leaders indicate depths of smear-slide samples. Because light and dark laminae were mixed together in the finely laminated mud sample from DE 8, we also show data for a typical light gray laminae from DE 10 in Core X and from a black laminae from DE 1 in Core S. Smear slides were analyzed semiquantitatively (e.g., Birks, 1981) using additional microfossil and plant fragment categories based on the system of Boulter (1994). Diatom data (black triangles show sampled depths) are explained by Hemphill-Haley and Lewis (2003).

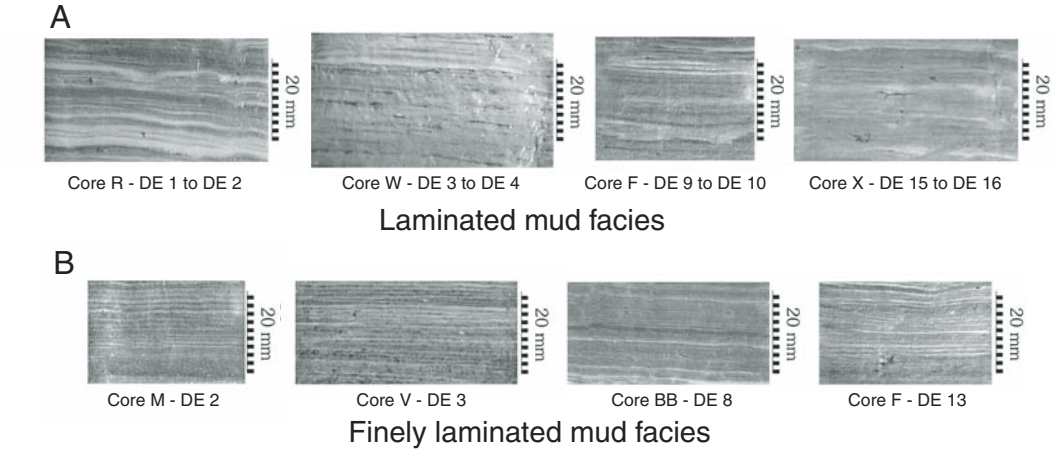

Figure 8. Photographs of 30-mm-thick sections of laminated mud facies (A) and finely laminated mud facies (B) from selected cores. Finely laminated mud facies cap disturbance event (DE) beds. Laminated mud facies occur between disturbance event beds.

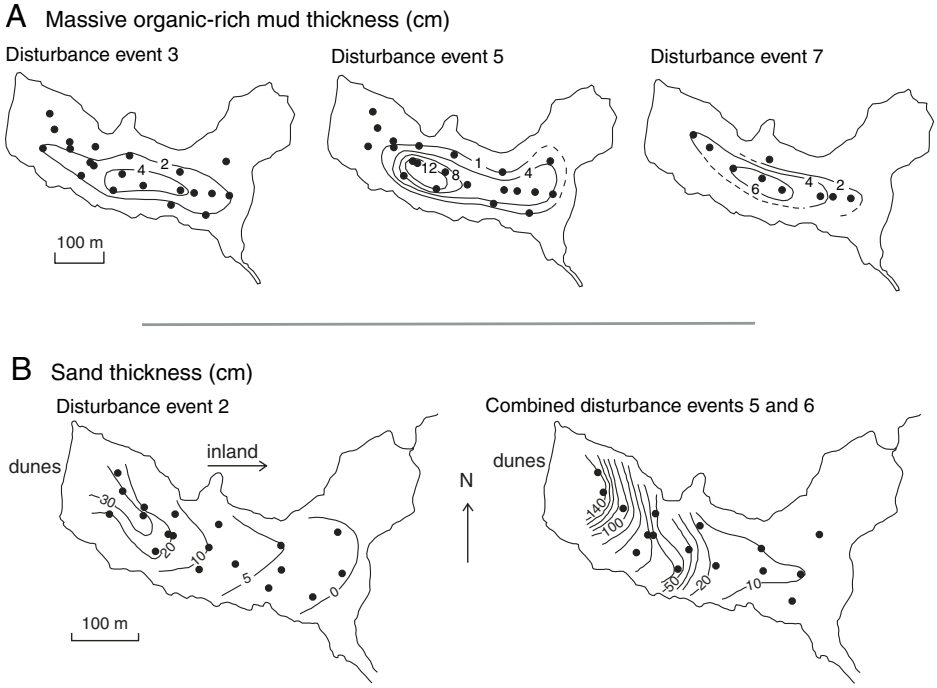

Figure 9. (A) Isopach maps showing thickness of the massive organic-rich mud facies for disturbance events 3, 5, and 7. (B) Isopach maps showing thickness of disturbance event 2 sand sheet and combined disturbance event 5 and 6 sand sheet.

from infrequent processes, such as turbidity flows, that affected limited areas of the lake bottom. Most massive mud facies were probably originally laminated but became structureless through erosion and redeposition by currents or by bioturbation. Massive sections at the top of cores (Fig. 4) reflect disturbance during coring or use of the lake as a log pond in the early twentieth century.

Massive Organic-Rich Mud Facies

The massive organic-rich mud facies contain more organic material (5%–11%) and more silt (40%–60%) than massive mud facies. Plant fragments are finer than those of debris-rich mud facies but coarser than fragments in laminated mud facies. Plant fragments fine upward in the massive organic-rich mud, and diatoms are relatively abundant near the tops. Underlying sand or debris-rich mud commonly grades into the massive organic-rich mud (Figs. 6 and 7). Locally, organic-rich mud either unconformably overlies erosional contacts or grades downward into underlying laminated mud facies.

We infer that the source of the massive organic-rich mud is sediment suspended throughout the water column following lake-wide disturbance events. Massive organic-rich mud facies thicken toward the deepest parts of the lake (Fig. 9A), indicating sediment focusing along the lake's axis during deposition.

Debris-Rich Mud Facies

Debris-rich mud facies contain conifer needles, twigs, deciduous leaves, and bits of wood intermixed with coarse silt and fine sand. Debris-rich mud ranges from <1 mm to tens of millimeters thick and in all cases grades upward into the massive organic-rich mud facies. Where sand beds are absent, debris-rich mud directly overlies erosive contacts. In sequences that contain multiple pulses of sand, debris-rich mud locally caps individual sand beds. Debris-rich mud facies occur in beds deposited during 13 of the 17 disturbance events. The coarse debris of debris-rich mud is the primary source of our ^{14}C samples. We infer that debris-rich mud results from the settling of coarse organic debris immediately following erosion of basal contacts and/or sand deposition during lake disturbance events.

Sand Facies

Sand is the basal lithofacies in the beds of 14 of the 17 disturbance events (Fig. 4; Table 2). The thickest sequence of sand beds in the western and middle portion of the lake were deposited by two disturbance events closely spaced in time. Emplacement of the sand of the later event (event 5) eroded away the entire thickness of the fine lake sediment that was deposited on top of the sand of the earlier event (event 6), resulting in an unusually thick sequence of sand beds (labeled "5/6" in Fig. 4). Only in cores X and M in the eastern (landward) part of the lake are thin beds of massive organic-rich mud well preserved between the sand beds of the two disturbance events.

We were able to penetrate the upper two thick sand layers in the west end of the lake (disturbance event 2 and combined disturbance events 5 and 6) (Fig. 4) using a vibracorer. In the central and eastern parts of the lake, the entire lake sediment column was penetrated. Sand layers associated with six disturbance events extend the entire length of the lake: events 2, 5, 6, 7, 8, and 12 (Table 2). In other cases, sand was only found in trace amounts in one core (events 3, 13, and 16) or as thin, 1–87-mm-thick layers in a few cores (events 1, 4, 10, 11, and 17, Table 2).

The sand beds of disturbance events 2, 5, and 6, which were found throughout the lake, were used for grain-size and thickness-trend analysis. These beds thin eastward away from the dune dam (Fig. 9B). The basal 40 mm of sand of disturbance events 2 and 6 is well sorted and medium fine (Fig. 10A). The weight percent of medium fine sand decreases eastward down the lake, and the weight percent of fine sand commensurately increases (Fig. 10B).

Sand beds have 1 to 13 fining-upward sequences (Figs. 4, 6, and 11; Table 3). Each sequence consists of medium fine sand overlain by fine sand, silt, or silty rip-up clasts. The grain-size transition was not gradual; medium fine sand commonly composed the bulk of a single sequence and was overlain abruptly by fine sand, silt, and/or rip-up clasts. Rip-up clasts occur at the top of the fining-upward sequences (Figs. 4 and 6) because they are less dense and hence more buoyant than sand grains. Rip-up clasts consist chiefly of laminated lake sediment (Fig. 6) and have long axis lengths up to 120 mm, with long axis length limited by the 75 mm core diameter. We infer that each fining-upward sequence marks a pulse of energetic deposition and that the fine silt or rip-up clasts at the top were deposited at the end of a pulse.

In general, the thicker the sand bed and the closer to the sand dune dam, the greater the number of fining-upward sequences (Figs. 4 and 11; Table 3). Whereas event 2 sand (maximum thickness = 36 cm) has a maximum of 2–5 pulses, combined events 5 and 6 sand (maximum thickness = 149 cm) has as many as 13 pulses (Table 3).

The fining-upward sequences within sand beds of combined events 5 and 6 can be cor-

TABLE 2. CHARACTERISTICS OF DISTURBANCE EVENT FACIES IN CORES FROM BRADLEY LAKE

Disturbance event	Number of cores[†]	Thickness of sand (cm)[‡]	Eastward extent of sand (m)[§]	Sand contains mud rip-up clasts	Sand has evidence of pulses[#]	Erosion at base (cm)[††]	Debris-rich mud thickness (cm)	Massive organic-rich mud thickness (cm)	Finely laminated mud thickness (cm)	Number of couplets of finely laminated mud[‡‡]	Max. conc. of Holocene marine diatoms[§§]	Bloom of brackish diatoms[##]
1	18	0–0.5	128 (B)	np	np	2.6	0–5.4	0.9–9.4	1.0–3.6	7–18	2.6	no
2	19	0–36	444 (O)	yes	yes	7.4	0.5–3.9	1.2–4.9	0.6–2.6	14–21	9.7	no
3	20	tr	244 (D)	np	np	unc	0.9–2.8	0.7–2.9	1.1–10.8	14–106	0	no
4	19	tr	284 (BB)	np	np	3.7	0.6–3.3	1.2–6.9	0.2–0.9	5–6	1.3	no
5	21	2.5–35	444 (O)	yes	yes	18.2	0.2–1.6	0.5–14.5	2.2–4.2	28–66	5.9	yes
6	2	0.5–118.4	417 (M)	yes	yes	**	0–1.6	0.5–3.4	0.8–1.2	5–22	1.2	yes
7	10	0.2–12.7	414 (F)	yes	yes	2.5	1.0–2.2	2.1–6.5	1.0–1.7	10–18	6.1	no
8	7	1.0–23.9	414 (F)	yes	np	2.5	0.9–1.9	0.9–5.3	5.0–6.5	41–78	9.0	yes
9	4	np	np	np	np	unc	np	0.3–0.9	0.9–1.8	11–20	0.9	yes
10	3	tr	284 (BB)	np	np	unc	np	4.2–6.0	0.8–2.2	14	0.45	no
11	4	tr	284 (BB)	np	np	2.5	0.7–1.1	2.1–4.7	2.8–4.1	47–57	1.8	yes
12	4	1.2–5.4	414 (F)	yes	np	4.5	0.3–2.6	3.3–3.9	5.0–6.9	56–66	14	yes
13	4	tr	284 (BB)	np	np	und	np	0.8–1.3	4.6–6.7	75–91	19	yes
14	4	np	np	np	np	unc	0.4–1.2	0.7–1.9	np	np	0	no
15	4	np	np	np	np	1.0	1.2–3.7	1.7–3.5	np	np	0	no
16	4	tr	379 (X)	np	np	yes	0.9–2.5	1.4–1.8	np	np	0	yes
17	4	0.2–8.7	414 (F)	yes	yes	yes	0.2–1.1	np	0.6–2.8	8–21	6.4	yes

Note: np, not present; tr, trace of sand in debris-rich mud facies; und, erosion occurred but minimum depth undetermined; unc, uncertain if any erosion occurred.

[†]Number of cores in which disturbance event was identified. The older disturbance events were reached only by Livingston cores E and F, and vibracores X and BB (Fig. 4).

[‡]Range in sand thickness among cores. For event 5, maximum thickness estimated in core V, where upper 35 cm of combined sand 5/6 are attributed to event 5 (see text). For event 6, maximum thickness is in core T, where upper 31 cm of combined sand 5/6 are attributed to event 5 (see text).

[§]Observed eastward extent of sand, including sand in debris-rich mud. For events 2, 5, 6, 7, and 8, we assume sand was deposited along the entire length of the lake because the easternmost core in which sand occurs (noted in parentheses) is the easternmost core that samples that event.

[#]Presence of depositional pulses of sand inferred from coarse-to-fine upward grading within sand beds (see Table 3).

[††]Minimum depth of erosion of underlying lake sediment (greatest value measured) based on correlation with disturbance events in cores M, O, or F at eastern end of lake. Disturbance event 5 erosion is the net erosion resulting from disturbance events 5 and 6.

[‡‡]Range in number of light-dark laminae couplets identified in finely laminated mud facies of corresponding disturbance event.

[§§]Maximum concentration of Holocene marine diatom valves (valves/cm^3 × 10^3) in disturbance event facies (Hemphill-Haley and Lewis, 2003).

[##]Maximum concentrations >10,000 valves/cm^3 constitute a bloom over background level counts (see Figs. 12 and 13).

related among cores V, T, W, H, and R in the western part of the lake (Fig. 11), and this correlation allows us to distinguish sand specific to disturbance event 5 from sand specific to disturbance event 6. Rip-up clasts generally occur in the lowest fining-upward sequences, are conspicuously absent in the middle fining-upward sequences, and reappear in the uppermost fining-upward sequences. We infer that sand specific to disturbance event 5 occurs in the uppermost fining-upward sequences that have rip-up clasts. The renewed influx of rip-up clasts is a product of erosion of the thin veneer of fine-grained lake sediment that was deposited on the floor of Bradley Lake in the few decades of quiescence after deposition of event 6 sand.

The lower contacts of basal sand beds deposited during disturbance events 2 and 6 are abrupt and locally truncate underlying laminations (e.g., Fig. 6B). The truncation and the laminated mud rip-up clasts (Fig. 6) testify to the erosive nature of the surge of water that carried sand into the lake. By correlating a prominent gray clay layer that is below the eroded base of sand from event 6, we measured the minimum depth of erosion (amount of missing section) at the base of the sand. Some erosion occurred at all core sites during this disturbance event, and erosion was 50–100 mm greater in the western half of the lake than in the eastern half. Erosion also was evident at the base of 12 of the other 16 disturbance events (Table 2); where it could be measured, erosion ranged from 10 to 74 mm.

Facies Associations

Based on their spatial relations and sequence in the cores, we group the seven lithofacies in Bradley Lake sediment into two facies associations. The first facies association consists of laminated, faintly laminated, and massive mud facies and includes most of the lake sediment section (Fig. 4). Based on detailed descriptions of two of the longest cores (cores E and BB, Fig. 4), 58% of the first facies association consists of laminated mud facies; the faintly laminated facies makes up ~20% of the first association. The remaining fraction of the first association consists mostly of massive mud facies with uncommon, short intervals of finely laminated mud facies. For the first association, we did not identify any regular pattern in the vertical sequence of lithofacies. We infer lithofacies of the first association to have been deposited by lake processes that vary seasonally in intensity with organic sedimentation predominant in the summer months and clastic sedimentation predominant in the winter months.

The second facies association includes distinct sequences of sand, debris-rich mud, massive organic-rich mud, and finely laminated mud facies irregularly interbedded within sediment of the first association (Figs. 4, 6, and 7). Although all facies of the second association are not present in each second-association sequence, the vertical sequence of facies is always the same. The sand facies almost always lies on an eroded contact and commonly contains rip-up clasts of underlying lake sediment (Fig. 6). Massive organic-rich mud, the most distinctive and widely distributed facies of the second association, occurs in almost every sequence of second-association beds in every core (Fig. 4; Table 2). Massive organic-rich mud usually overlies sand and debris-rich mud; but in the eastern half of the lake, where sand facies are thin or absent, organic-rich mud facies commonly disconformably overlie laminated mud of the first facies association. Finely laminated mud facies cap the second

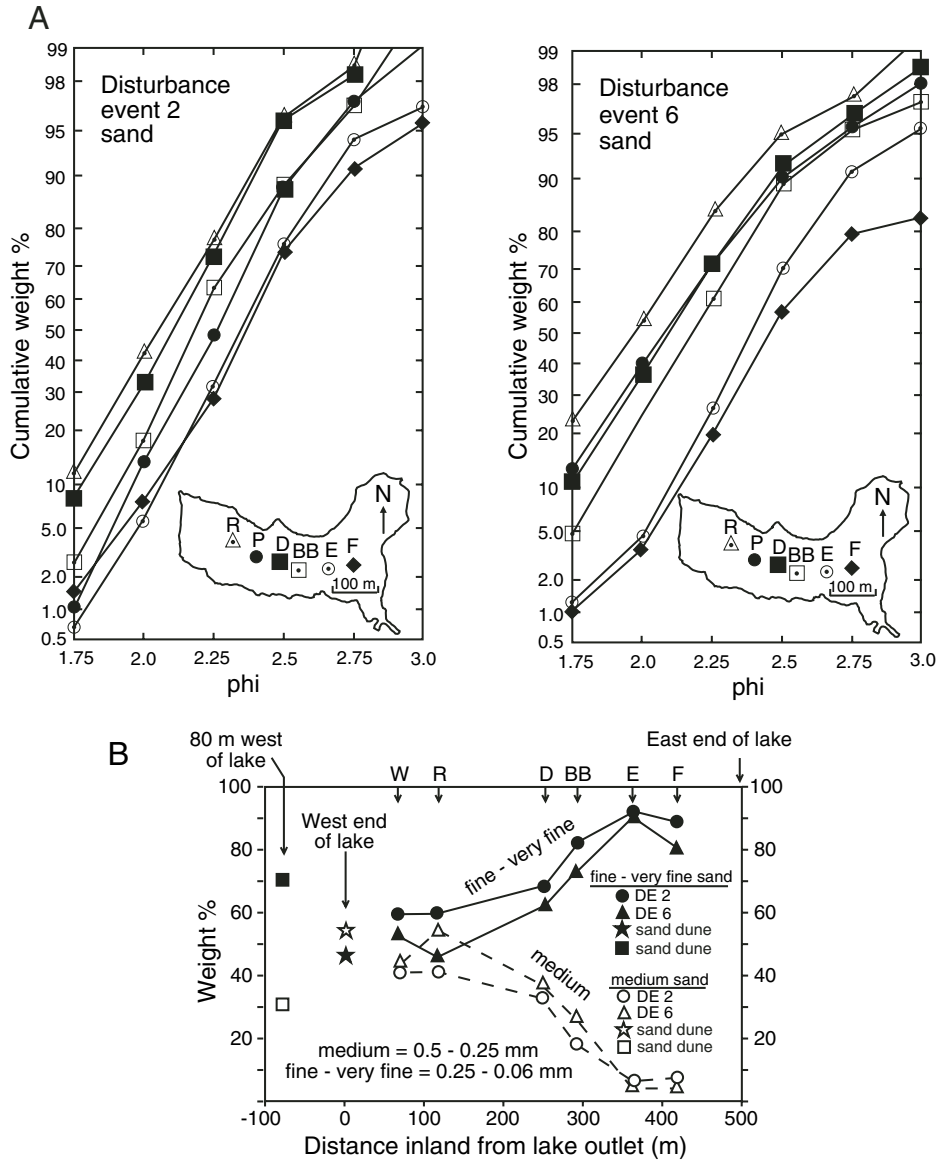

Figure 10. (A) Grain-size distributions for basal disturbance event 2 sand and basal disturbance event 6 sand in cores that are at increasing distances from the ocean (R, P, D, BB, E, and F are core sites, with "R" most oceanward and "F" most landward). Both basal sand units become generally finer going away from the ocean. Most of the basal sand is within the fine-sand range (2.0–3.0 phi). For plotting purposes, particle sizes were truncated at 1.75 phi at the coarser end and 3.0 phi at the finer end. (B) Grain-size trends for medium sand and for fine-to-very-fine sand going from the dune 80 m west of Bradley Lake eastward to core F in the lake.

association and commonly grade upward into overlying laminated mud facies of the first association (Figs. 4, 6, and 7). Based on the lithology, bed contacts, sedimentary structures, and lake-wide extent, we infer that facies of the second association were deposited during and after infrequent disturbance events that severely disturbed and temporarily changed sedimentation over the entire lake bottom.

DIATOM BIOSTRATIGRAPHY

Diatoms preserved in the lake sediment indicate that Bradley Lake has always been a freshwater lake (Hemphill-Haley, 1996; Hemphill-Haley and Lewis, 2003). An overwhelming abundance of freshwater diatoms (~99.8% of all diatoms) throughout the lacustrine strata indicates that Bradley Lake never had an open connection with the ocean. Freshwater diatoms consist of benthic floras that live in shallow areas along the shores of the lake (~8% of lake surface area, Fig. 3) and planktonic species that live in the upper few meters of the water column. Although the lake has always supported an abundance of freshwater diatoms, their concentrations are reduced following disturbance events (Figs. 12 and 13). The entirely freshwater diatom biofacies almost always coincides with lithofacies of the first association (laminated, faintly laminated, and massive mud facies) and coincides with some of the finely laminated mud facies.

Rare fossil marine diatoms in Bradley Lake strata are evidence for marine incursions during disturbance events. Where fossil marine diatoms are present, they are three to four orders of magnitude less abundant than the prolific freshwater diatoms (Figs. 12 and 13). Marine diatoms consist of three types (Hemphill-Haley and Lewis, 2003): (1) extinct Miocene-Pliocene species eroded out of diatomites that partially underlie the lower China Creek valley (Whiting and Schrader, 1985); (2) marine diatoms that are found both in the diatomite and in modern coastal deposits; and (3) Holocene marine diatoms that consist of marine species from modern coastal deposits not found in the diatomite. With few exceptions, Holocene marine diatom biofacies in Bradley Lake strata coincide with those lithofacies associated with disturbance events, that is, with the second facies association of sand, debris-rich mud, massive organic-rich mud, and finely laminated mud (Figs. 12 and 13). Holocene marine diatoms did not live in the lake; they were imported to the lake during marine incursions.

Brackish diatoms are always present in Bradley Lake at background levels but bloom immediately after disturbances. Brackish diatom biofacies locally increase rapidly in numbers in the finely laminated mud at the top of certain disturbance event intervals (Figs. 12 and 13; Table 2). Based on the number of light-dark laminae couplets in the finely laminated mud, brackish diatom blooms can persist for a few years to several decades (Table 2). The composite range of salinity tolerance for the three reported species of brackish diatoms (Carpelan, 1978; John, 1983; Cumming and Smol, 1993; Fritz et al., 1993; Wilson et al., 1996) (Fig. 13) suggests that blooms resulted from lake salinities up to ~4 g/L (4‰). Blooms of *C. meneghiniana* and *T. bramaputrae* are known to be stimulated by increased salinity (Foged, 1981). However, other paleoecological factors can prompt blooms of *C. meneghiniana,* including expansion of epiphytic habitat, increased

turbidity, and greater availability of nutrients (S.C. Fritz, 2002, personal commun.).

DATING DISTURBANCE EVENTS

Approach

Although ^{14}C dating is our primary means of dating disturbance events, it is rarely capable of distinguishing events that differ in age by less than hundreds of years. We use two additional techniques to increase the precision of our ages for disturbance events. First, independently derived sedimentation rates verify ^{14}C-based estimates for the number of years between disturbance events. The independent rates come from counting light-dark couplets in finely laminated mud facies, which we assume to be varves. Second, we use the program OxCal (Bronk Ramsey, 1995, 2001), based on Bayesian statistical methods, to evaluate the stratigraphic consistency of ^{14}C ages. The program helps select ^{14}C ages or groups of ages that provide the most internally consistent estimates for the times of disturbance events. When combined with varved-based sedimentation rates for intervals between disturbance event beds, the precision of OxCal-derived ages for disturbance events increases by as much as 100%.

Selection of Detrital Macrofossils for ^{14}C Dating

We dated beds of the 17 disturbance events in Bradley Lake with 61 AMS ^{14}C ages (Table 4) measured on detrital plant fragments from 12 cores (Tables 4 and 5). Because the dated fragments came from sand, debris-rich mud, or coarse-grained, organic-rich mud facies, most fragments were probably deposited within a time span of a few hours. The fragments were probably derived from highly unconsolidated organic-rich sediment deposited in shallow water along the margins of the lake, which slumped or was suspended during disturbance events.

Although terrestrial macrofossils are the preferred material for ^{14}C dating lake sediments (Hedges, 1991; Wohlfarth et al., 1998), many dated samples contained stems of the aquatic moss *Fontinalis* sp. (J.A. Janssens, 1999, personal commun.) (fragment type B, Tables 4 and 5). In lakes with a significant carbon reservoir effect, aquatic plant fossils yield ^{14}C ages much greater than similar-aged terrestrial fossils (Hedges, 1991). Any such effect in Bradley Lake is apparently insignificant because the ages on samples with few or no stems show no systematic age difference from those with many stems from the same disturbance events (Table 4). A few samples contained small portions of rootlets or papery root sheaths, some of which could be aquatic; however, laminations throughout the dated cores show that the lake was almost always too deep for aquatic plants to root in the central, cored part of the lake.

All dated samples are detrital (Table 4; Table DR1, see footnote 1) and, therefore, sample ages may predate deposition by an unknown number of years. To minimize the time difference between plant (rarely animal, Table 4) death and fragment deposition, we selected fragments that were least likely to be reworked. Fragments of deciduous tree or shrub leaves, well-preserved parts of herbaceous plants (stems, leaves, buds,

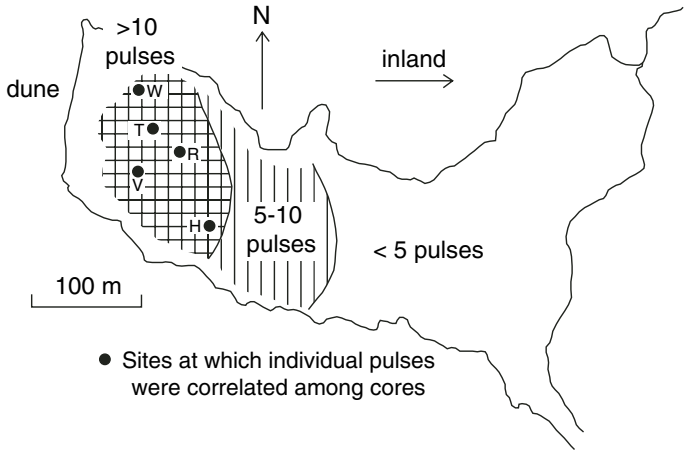

Figure 11. Number of depositional pulses within combined disturbance events 5 and 6 sand. H, R, T, V, and W are core sites.

TABLE 3. SAND THICKNESS AND NUMBER OF FINING-UPWARD PULSES IN CORES FROM BRADLEY LAKE

Core†	Disturbance event 2‡			Combined disturbance events 5 and 6‡		
	Sand thickness (cm)	Minimum number	Maximum number	Sand thickness (cm)	Minimum number	Maximum number
V	16.0	2	3	136.0	7	9
T	36.0	2	3	149.4	12	13
W	27.0	1	2	138.9	10	11
B	35.0	2	3	#	#	#
R	19.7	1	1	108.6	9	10
H	26.0	2	5	73.3	8	10
C	25.0	2	3	75.5	4	≥5††
P	14.0	2	2	53.5	7	9
G	21.8	1	2	58.1	6	7
J	8.8	1	1	60.0	5	7
D	9.6	2	2	43.3	6	6
I	6.7	2	2	11.5	4	5
BB	0.6§	1	1	14.6	3	4
L	4.7	2	3	7.5	2	3
E	1.4	1	1	16.1	3	4
K	6.7	2	2	10.3	3	4
X	§	§	§	10.0	3	3
N	1.5	1	2	3.3	2	3
F	1.3	2	2	14.8	3	5
M	1.3	1	1	3.0	2	2
O	1.0	1	1	2.5	3	3

†Cores are listed in descending order from most seaward.
‡Maximum and minimum number of fining-upward pulses were counted because of instances where it was uncertain whether a fining trend was actually a separate pulse or only apparent because of the presence of a rip-up clast in the middle of a fining interval.
§The uppermost meter of cores X and BB is severely compacted.
#Core B did not penetrate deeply enough to fully sample disturbance event 5 sand.
††Disturbance due to coring precluded an estimate of the maximum number of pulses.

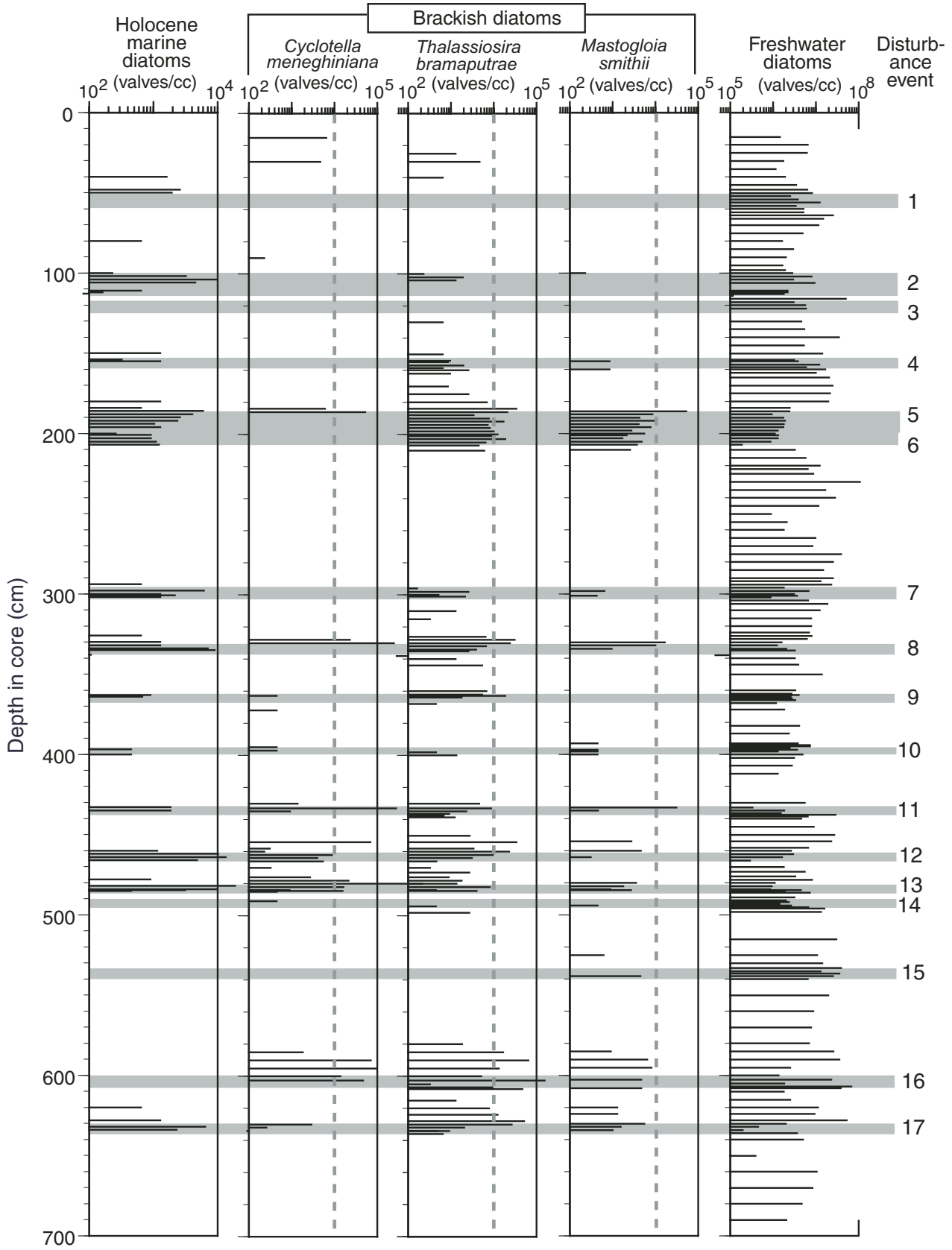

Figure 12. Concentrations of marine, brackish and freshwater diatoms for disturbance event 1 through disturbance event 17. Vertical dashed lines for brackish diatoms show an estimated delineation between background occurrences and large increases in growth of these taxa. Data are from cores E, F (90–100 cm), BB (360–412 cm), and X (473–498 cm).

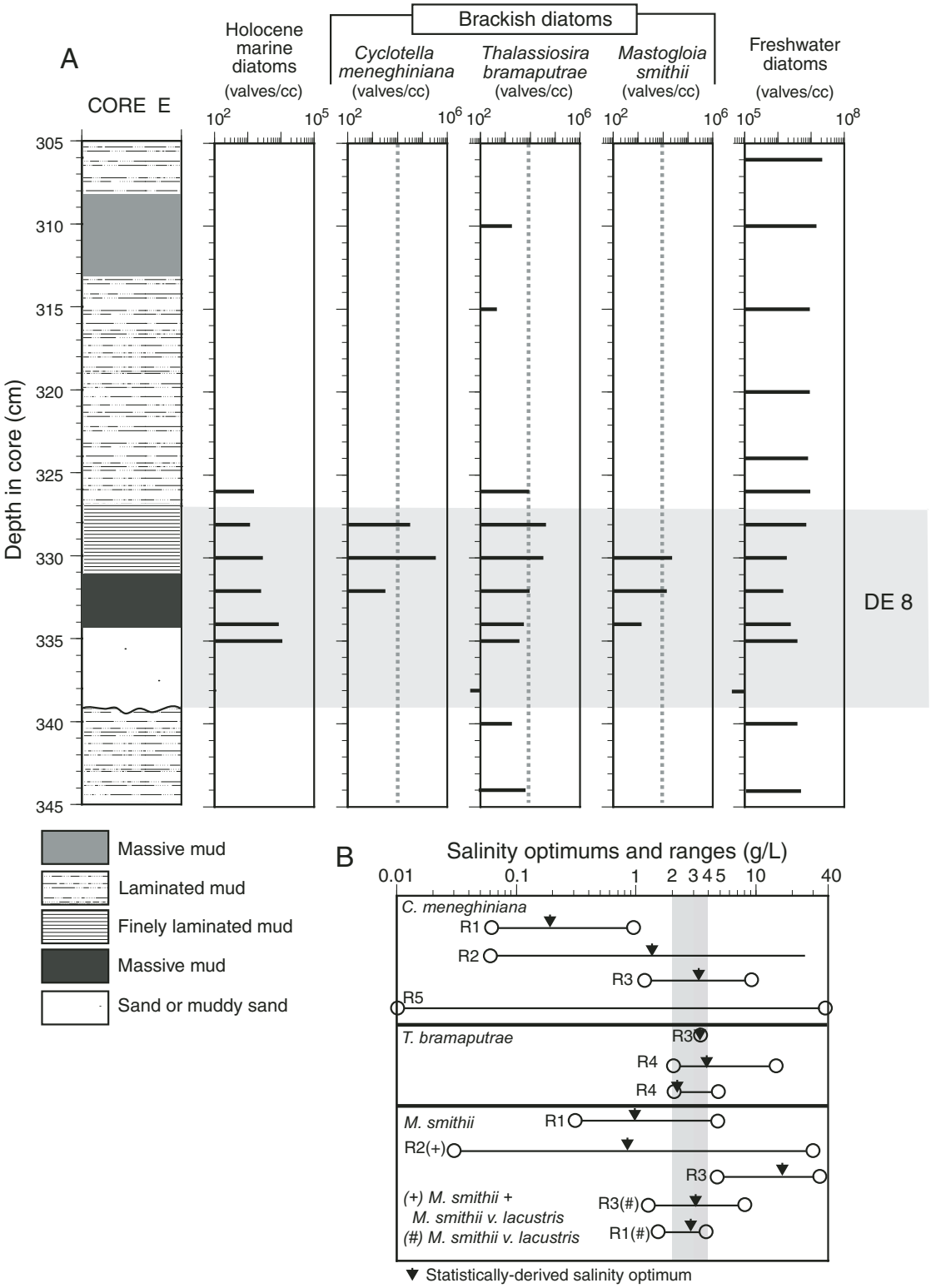

Figure 13. (A) Expanded view of disturbance event 8 (DE 8) in core E showing that Holocene marine diatoms increase in the upper part of the sand and the overlying massive organic-rich mud. The brackish group of diatoms increase in the top of the massive organic-rich mud and the overlying finely laminated mud at the same time that overall abundances of freshwater diatoms (both benthic and planktonic) are suppressed. (B) Inferred salinity ranges for brackish diatoms from Bradley Lake, based on modern occurrences in lakes and estuaries. Key to references: R1—Cumming and Smol (1993); R2—Wilson et al. (1996); R3—Fritz et al. (1993); R4—John (1983); R5—Carpelan (1978).

TABLE 4. AGES FOR DISTURBANCE EVENTS AND RADIOCARBON DATA FOR DETRITAL MACROFOSSILS IN BRADLEY LAKE

Event†	OxCal age (cal yr B.P. at 2σ)‡	Calibrated age (cal yr B.P. at 2σ)§	Lab-reported age (^{14}C yr B.P. at 1σ)#	Radiocarbon laboratory number	Core number	Depth in core (m)††	Reworking class‡‡	Proportions of fragment types§§
DE 1	250 (assumed)	440–0	230 ± 50	AA-17130	E	0.59	C	2H, 2R, 1N, B
		510–300	360 ± 60	CAMS-12825	C	0.39	B	3S, 2B
		560–330	460 ± 45	AA-17138	F	0.50	C	2N, 2H, 1B, S, T
		Not used	1120 ± 110 R	AA-20159	BB	0.45	B	2H, 2R,1B, L
DE 2	1000–920	**1060–920***	1030 ± 60*	CAMS-12288	C	0.85	C	1H, 1N, 1B, 1T, 1R
			1085 ± 70*	AA-19302	F	1.03	C	4B, 1T, 1N, I
			1095 ± 50*	AA-20175	E	1.05	A	2H, 1L, 1B, 1R, T, S, I
		1290–1060	1265 ± 55 R?	AA-17126	C	0.78	D	3T, 2R
		Not used	1780 ± 110 R	AA-20160	BB	0.79	C	2T, 1L, 1H, 1B, R
DE 3	1130–980	**1170–930***	1100 ± 45*	AA-23209	N	0.97	A	2S, 1B, 1H, 1I
			1150 ± 120*	AA-20176	E	1.24	B	2H, 1B, 1S, 1W, I, L, N, R
		1390–1170	1360 ± 55	AA-23206	D	1.34	A	3B, 1L, 1I
DE 4	1420–1310	**1520–1310***	1600 ± 100*	AA-20161	BB	1.01	C	2R, 1H, 1I, 1B, O, L, T
			1530 ± 45*	AA-23210	O	1.09	B	4B, 1L, I
			1495 ± 45*	AA-23208	I	1.55	B	2B, 2H, 1I, L
			1480 ± 45*	AA-20177	E	1.61	B	1H, 1R, 1S, 1B, 1O, N, L, I, W
DE 5/6	1810–1600	**1820–1600***	1610 ± 80*	CAMS-13056	C	2.35	D	5R
			1780 ± 35*	OS-27153	N	1.47	D	5R
	(light-dark couplets		1792 ± 30*	OS-27154	D	2.23	D	5R
	suggest that	2010–1630	1915 ± 70	AA-17127	C	2.05	C	2R, 2B, 1S
	DE 5 and 6 differ	2330–2000	2160 ± 55	AA-17128	C	2.63	E	2C, 2T, 1R
	in age by >22 yr)	2150–1710	1985 ± 85	AA-17131	E	2.04	E	5T
		2310–2000	2150 ± 45	AA-23207	H	2.58	A	4B, 1I
		2150–1920	2070 ± 45	AA-23217	X	1.95	A	5B
		2750–2150	2325 ± 60	AA-20162	BB	1.36	B	2B, 1L, 1O, 1H, R, I
DE 7	2860–2740	**2860–2750***	2670 ± 60*	AA-19300	E	3.00	C	3B, 2N
			2695 ± 45*	AA-26598	P	3.24	A	5B
			2735 ± 95*	AA-20163	BB	2.15	B	2B, 1I, 1O, 1H, L, S
		2720–2350	2440 ± 50	AA-20164	BB	2.15	D	5N
		3210–2850	2870 ± 55	OS-27152	I	2.70	D	5R
		Not used	3205 ± 70 R	AA-20165	BB	2.15	E	5W
DE 8	3270–3090	**3260–2990***	2960 ± 60*	AA-20166	BB	2.55	D	5R, O, B, S
			2950 ± 50*	AA-23213	X	3.19	A	3L, 2B, I
			2970 ± 70*	AA-20178	E	3.34	D	3N, 1T, 1O, R, B, L, H, I
DE 9	3410–3240	**3470–3240***	3090 ± 100*	AA-26596	BB	2.73	B	3H, 1L, 1O, R, C
			3160 ± 55*	AA-26595	X	3.29	C	1S, 2H, 1R, 1N, C, O, L
DE 10	3830–3640	**3840–3630***	3430 ± 60*	AA-20167	BB	3.09	D	4N, 1H, L, R, O
			3480 ± 50*	AA-23212	X	3.64	B	2I, 1H, 1L, 1B
DE 11	4240–4080	**4350–4080***	3790 ± 90*	AA-20168	BB	3.49	B	2H, 1B, 1I, 1R, S, N
			3815 ± 50*	AA-20181	X	4.02	B	2O, 1H, 1N, 1B, R, S, T, L, I
			3805 ± 50*	AA-20179	E	4.39	C	3N, 1H, 1O, R, B, L, S
DE 12	4420–4260	**4420–4150***	3985 ± 55*	AA-20182	X	4.29	C	2N, 1L, 1H, 1T, B, R, S
			3840 ± 65*	AA-17139	F	4.43	E	5T
			3795 ± 60*	AA-17132	E	4.70	E	5T
		4870–4520	4190 ± 75 R?	AA-20169	BB	3.75	D	2N, 2R, 1B, H
DE 13	4630–4460	**4790–4400***	4135 ± 75*	AA-20183	X	4.49	B	2H, 1L, 1R, 1B, S, T, I
			3965 ± 50*	AA-26597	E	4.86	C	1C, 1H, 1L, 1N, 1R, O, S
		5050–4600	4305 ± 65 R?	AA-20170	BB	4.01	C	2R, 1N, 1I, 1H, O
DE 14	4730–4530	**4830–4550***	4180 ± 60*	AA-20171	BB	4.10	B	3H, 1N, 1I, R, O, B
			4150 ± 55*	AA-20180	E	4.96	A	2L, 1N, 1H, 1O, T, S, B, R
DE 15	5600–5320	**5600–5320***	4780 ± 50*	AA-26599	BB	4.66	B	2H, 2L, 1B, O, R, S
			4735 ± 75*	AA-20172	BB	4.67	A	2H, 1L, 1I, 1O, R, B
		Not used	5295 ± 55 R	AA-17135	E	5.41	E	5T
DE 16	6510–6310	**6510–6310***	5625 ± 55*	AA-20173	BB	5.28	C	2H, 1L, 1N, 1C, R, S, I, W
			5635 ± 60*	AA-23215	X	5.69	C	2N, 1H, 1B, 1L, R
			5725 ± 70*	AA-19301	E	6.09	A	3H, 2L
DE 17		**7430–7260***	6325 ± 65*	AA-20174	BB	5.58	C	2N, 2H, 1O, L, R, B, S, T, I
			6480 ± 60*	AA-23216	X	5.89	B	5H
Peaty		7670–7430	6675 ± 70	AA-17136	E	6.37	D	3S, 2T
mud		7840–7580	6870 ± 65	AA-17137	E	6.69	C	3S, 2R
		7960–7670	7005 ± 80	AA-17140	F	6.69	B	2L, 2H, R

Note: Selected fragments of plants (rarely animals) retained on a 0.5 mm sieve, scraped with dental tools under a binocular microscope at 6–25×, and repeatedly rinsed with distilled water. Fragment types in last column of table. Additional data in Table DR1 (see footnote 1).

†Disturbance events (DE) as numbered on figures and explained in text. DE 5 and 6 could be separately identified in only two cores (M and X); ^{14}C samples are from other cores where the two disturbance events are grouped as DE 5/6. Freshwater peaty mud lies below lake sediment in cores E, F, X, and BB.

‡Ages (cal yr B.P.; 2σ) for each disturbance event obtained with the "V-sequence" feature of OxCal (version 3.4, Bronk Ramsey, 2001) using the calibrated ages shown in bold one column to the right and estimates (and 1σ errors) of time intervals between disturbance events calculated from sedimentation rates and mean sediment thicknesses for intervals between disturbance events in cores P, M, J, D, C, X, F, E, and BB. Sedimentation rates based on light-dark couplet counts within finely laminated mud facies in DE 2–9 successions and assumed uniform sedimentation rates for DE 9–14 (0.83 ± 0.17 mm/yr) and DE 14–16 (0.46 ± 0.23 mm/yr; Fig. 14; Table DR2, see footnote 1).

§Ages calculated using OxCal (version 3.4, Bronk Ramsey, 2001) and the INTCAL98 data set of Stuiver et al. (1998). Dating laboratories state that no additional interlaboratory variance (error multiplier; e.g., Taylor et al., 1996) is required for calibration of ages; results from these laboratories in the Third International Radiocarbon Comparison show minimal interlaboratory variance. Calibrated ages show time intervals of >95% probability distribution at 2σ. Bold ages are calibrated from the means of the ages marked with an asterisk within each disturbance event. Ages used for means meet chi-squared criteria at the 95% level (OxCal combined ages).

#AMS (accelerator mass spectrometer) ^{14}C ages reported by radiocarbon laboratory (^{14}C yr B.P.). Quoted error for each AMS age is the larger of counting error or target reproducibility error. "R" marks samples so old that they must contain fragments that are reworked. "R?" marks samples that contain fragments that are probably reworked. Asterisk marks ages that are averaged in the column to the left. Age of 1792 ± 30 for DE 5/6 is the mean of two ages on the same root fragment.

††Listed depths are not corrected for compaction or possible missing section.

‡‡Five-class scale of likelihood of reworking as explained in Table 5. The most delicate fossils, which probably have the least chance of being reworked, are labeled "A." Wood and charcoal are labeled "E."

§§Types of plant (rarely animal) fragments in dated samples as explained in Table 5. Numbers indicate approximate proportions of different fragment types in fifths; types with no number make up <10% of sample.

small rootlets), and the common, delicate stems of *Fontinalis* sp. were the preferred sample material because such parts decay rapidly and are unlikely to be reworked. We avoided highly decayed plant parts and fragments of wood or charcoal and used conifer seeds and needles sparingly, because these materials are more resistant to decay and so more likely to be reworked. Because of size requirements for routine ^{14}C samples, most samples consist of mixtures of different types of plant fragments (Table 4; Table DR1, see footnote 1).

Fragments in each sample were selected from the 0.5-mm-sieve fraction of 5–20-mm-thick samples of core sediment. Highly decayed tissue and sediment were scraped from fragments with dental tools at 6-to-25-times magnification in distilled water before samples were dried and submitted for AMS analysis. Although cores and samples were stored at 4 °C for as long as 3 yr before cleaning of submitted samples, no contamination effects (e.g., Wohlfarth et al., 1998) are apparent in comparisons of ages on materials prepared in different years.

TABLE 5. TYPES OF ORGANIC FRAGMENTS IN ^{14}C DATED SAMPLES AND ASSIGNED SAMPLE REWORKING CLASS

Fragment type	
B	Thin (<0.5 mm diameter), dark brown, barbed stems of aquatic moss (*Fontinalis* sp.)
C	Unabraded fragments of charcoal and charred wood
H	Large, nonwoody buds or stem-like fragments of herbs
I	Unabraded, brown, translucent fragments of insects, seed cases, or other papery herb parts
L	Fragments of leaves of herbs, shrubs, or deciduous trees
N	Conifer leaves (needles) and buds, chiefly spruce, cedar, Douglas fir, and hemlock
O	Undecayed fragments of plants and animals not included in other types
R	Unabraded, nonwoody fragments of roots and rootlets, including papery root sheaths
S	Herbaceous seeds or seed cases
T	Twigs, parts of conifer cones, woody herb stems, and woody rootlets
W	Unabraded fragments of wood
Likelihood of reworking class†	
A	Undecayed, deciduous tree leaves and soft fragments of herbs, such as leaves, buds, small stems, and small rootlets
B	Mixtures of fragments of class A and larger nonwoody stems, insect parts, herb seeds, nonwoody rootlets, and other undecayed soft parts of plants and animals
C	Mixtures of fragments mostly from classes B and D
D	Undecayed conifer leaves, soft woody herb stems, and delicate cone bracts; includes some moderately decayed fragments from classes A, B, and C
E	Wood fragments, woody rootlets, twigs, large seeds or bracts, charcoal, and decayed woody herb parts and conifer leaves, particularly those encrusted with vivianite

†We used the proportions (in fifths, Table 4) of the various types of fragments and the degree of decay of fragments to classify each sample. For example, samples consisting primarily of little-decayed leaves or delicate parts of herbs were classified "A" (least chance of reworking), whereas those with much wood, charcoal, twigs, or parts of woody rootlets were classified "E" (greatest chance of reworking).

Evaluation of Ages

All but 6 of the 61 ^{14}C ages from Bradley Lake (Table 4) are in correct stratigraphic order, suggesting that most components in the dated samples do not predate times of deposition by more than a few hundred years. Similarly, the uniform sedimentation rate indicated by the depth distribution of most of the ages for the past 4000 yr (Fig. 14) is inconsistent with ages on samples consisting of materials of widely differing age.

Seven ages are best explained by the reworking of older detritus into the center of the lake. The most obvious outliers are single ages from each of disturbance events 1, 2, 7, and 15 (labeled "Not used" on Table 4); each of these ages is 2.5–5 standard deviations older than the next nearest age (^{14}C yr). Other single ages in disturbance events 2, 12, and 13 (labeled "R?") are older than the other ages from the same disturbance event. But because their calibrated-age distributions (at 2σ) overlap with the distributions of at least the next oldest age, these age relations may result only from statistical plus age variations resulting from variable ^{14}C production in the upper atmosphere over time (DeVries variations, e.g., Taylor et al., 1996; Stuiver et al., 1998). More likely, some of the fragments in these samples are significantly older than others, yielding an older ^{14}C age than other samples from the same disturbance event. In the clearest example of sample components of different age, three ages on different materials picked from the same sample from disturbance event 7 differ by as much as 500–1000 ^{14}C yr (2σ).

Anomalously young ages are more difficult to explain. The calibrated, 2σ age distribution for the youngest age from disturbance event 7, on well-preserved spruce needles, almost overlaps with the distribution for the next youngest ages for that disturbance event and, therefore, its anomalously young age may reflect only statistical plus DeVries variations. The alternative interpretation, which is that this anomalously young age is the most accurate age for disturbance event 7 and that other ages are on reworked fragments, receives little support from the following stratigraphic sequence analysis.

To increase the precision of our estimates for the times of each disturbance event we use the program OxCal (Bronk Ramsey, 1995, 2001) with the INTCAL98 radiocarbon calibration data set of Stuiver et al. (1998; Table 4) in two ways. First, uncalibrated ^{14}C ages from the same disturbance event that are similar enough to be considered from the same population at the 95% level (using a chi-squared test) are averaged to obtain a mean age with a standard deviation smaller than the deviations of the averaged ages. Secondly, the sequence analysis feature of OxCal compares the age distributions of all calibrated mean and unaveraged ^{14}C ages in stratigraphic order to evaluate the stratigraphic consistency of each age in relation to ages above and below it. The program then reports a probability, which is a measure of the degree to which each calibrated age is stratigraphically consistent with adjacent ages. Low probabilities highlight ages that are inconsistent with other ages for a disturbance event or with ages for underlying or overlying events.

For our OxCal analyses, we placed ages (except "Not used," Table 4) into 19 groups (17 disturbance events plus a clast of marsh peat and the basal freshwater peat; Fig. 4) in stratigraphic order, with the ages in each group unordered. Because the sequence analysis reported that the ages labeled "R?" (Table 4) in disturbance events 2, 12, and 13 had low probabilities (<8%) of being in the correct stratigraphic order, we eliminated them. Retained ages and mean ages (56 of the original 61 ages) had high probabilities of being in the correct stratigraphic order (>98%).

We also used OxCal to evaluate the consistency of ages in the different reworking classes of Tables 4 and 5. The analysis showed only that ages on charcoal and wood are less stratigraphically consistent than those on more delicate materials.

Constraining Event Ages with Sedimentation Rates

The uniform sedimentation rates characteristic of small, temperate-climate lakes in forested areas (Oldfield, 1977; O'Sullivan, 1983) provide a means of further evaluating and increasing the

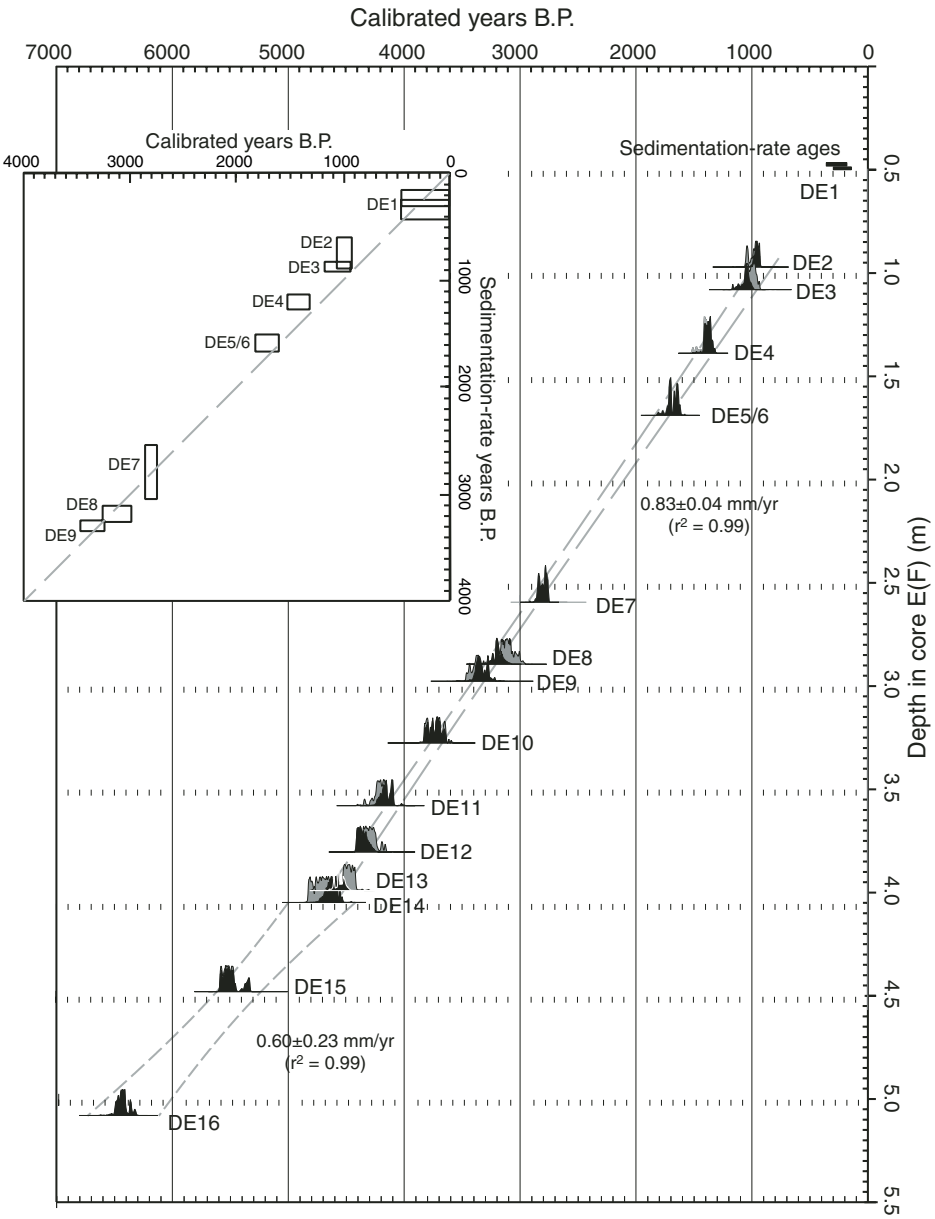

Figure 14. Calibrated-age (yr before A.D. 1950) distributions for disturbance events (DE) in Bradley Lake determined with the program OxCal (Bronk Ramsey, 1995; 2001). The range of initial distributions (gray) were narrowed (final black distributions) using estimates of the number of years between disturbance events derived from sedimentation rates (Table DR2, see footnote 1). Disturbance events 5 and 6 cannot be distinguished with ^{14}C ages and so are grouped together (DE 5/6). Dashed lines show 95% confidence limits on sedimentation-rate regression lines fitted through the ^{14}C calibrated-age distributions for DE 2 to DE 14 and DE 14 to DE 16. Inset diagram shows how calibrated ^{14}C ages (Table 4) compare to ages derived from sediment thickness and sedimentation rates. The greater of the two sedimentation-rate ages shown for DE 1 is a maximum age (Fig. DR2, see footnote 1).

precision of the ages of disturbance events with OxCal. We estimate the absolute number of years between disturbance events from sediment thicknesses between events and sedimentation rates derived from counting varves in the finely laminated mud facies of disturbance events (Table DR2, see footnote 1). When the number of years (with errors) for each interval are added to the sequence analysis feature of OxCal, the program recalculates the probabilities of ^{14}C ages being stratigraphically consistent and commonly narrows the range of the OxCal-derived age distributions for disturbance events based on the minimum and maximum number of years between events.

Sediment thicknesses in the axial lake cores (cores C, D, E, F, J, M, P, X, and BB; Table DR2, see footnote 1) are corrected for erosion during disturbance events and for compaction during vibracoring. By correlating distinctive gray laminae beneath the erosional contact of each disturbance event, we estimate the depth of lake-bottom erosion at most core sites during each disturbance event relative to the least-eroded cores (M, O, or F) at the eastern end of the lake (Table 2). Compaction in the upper few meters of vibracores is corrected through comparison with uncompacted piston cores.

To estimate sedimentation rates for each corrected thickness of sediment between disturbance events, we counted the number of varves (light-dark couplets) within the finely laminated mud facies of each core in which they were well preserved. Finely laminated mud facies ranged from 10 to 70 mm in thickness. We then determined an average sedimentation rate for the finely laminated mud beds above each disturbance event by averaging rates for beds above each disturbance event in each core. Standard deviations on average rates ranged from 15% to 31%. Finally, we estimated the sedimentation rate for each interval of sediment between disturbance events by averaging the rates for the finely laminated mud beds at the base and top of each interval (Table DR2, see footnote 1).

We also counted gray laminae in intervals where they were well preserved to obtain an independent minimum estimate of the number of years between disturbance events. Due to some indistinct laminae and minor postdepositional disturbance in all intervals, even counts in intervals with the most distinct gray laminae (24 counts in 11 intervals in 8 cores) are less than all but three of the minimum-year estimates obtained from sedimentation rates: those for the disturbance event 2–3, disturbance event 3–4, and disturbance event 5–6 intervals. For these intervals, we increased the minimum-year estimates by 12–15 yr to match our counts.

Sedimentation rate ages for disturbance events 2–9, derived by summing the number of years for each interval obtained from sedimentation rates (Table DR2, see footnote 1), compare favorably with the ^{14}C ages for the same disturbance events (Fig. 14). The consistency in the two types of independently calculated ages for disturbance events supports our assumptions that gray laminae in laminated mud facies are no more frequent than annual and that light-dark couplets in finely laminated mud facies are varves.

Sedimentation rates from finely laminated mud facies of the youngest interval of lake sedi-

ment (lake sediment–water interface to base of finely laminated mud facies of disturbance event 1) yield more accurate ages for disturbance event 1 than its ^{14}C ages. Due to wide fluctuations in the radiocarbon calibration curve for the past few hundred years (Stuiver et al., 1998), the ^{14}C ages show only that disturbance event 1 is less than 440 cal yr B.P. (calibrated years before A.D. 1950; Table 4). Counts of light-dark couplets in 10–20-mm-thick intervals in the middle of the youngest interval in eight cores yield sedimentation rates of 1.8 ± 0.25 mm/yr. This rate combined with the average core thickness (Table DR2, see footnote 1; 485 mm) yields an age of 226 ± 76 yr B.P. (2σ). A less accurate age estimate for disturbance event 1 (325 ± 94 yr B.P.) was obtained by using sedimentation rates to model the natural compaction gradient in the interval from the sediment interface to disturbance event 2 (Fig. DR1, see footnote 1). Both sedimentation-rate ages for disturbance event 1 (Table 4; Fig. 14) encompass our later correlation of this event with the tsunami accompanying the great Cascadia earthquake of 26 January A.D. 1700 (Satake et al., 1996, 2003).

Sedimentation-rate-based time intervals between disturbance events are much less certain for intervals between disturbance events 9–17 than for younger intervals. Only four cores (E, F, X, and BB) penetrate disturbance events 9–17, and the finely laminated mud facies of these disturbance events are less well preserved than the facies in younger disturbance event sequences. We estimated the number of years between predisturbance-event-9 events by assuming constant sedimentation rates obtained from linear regressions through age-depth plots for disturbance events 2–14 and disturbance events 14–16 (Fig. 14). A 5% (±0.04 mm/yr) error on the rate derived from the disturbance event 2–14 regression was arbitrarily increased to 20% (0.83 ± 0.17 mm/yr) to approximate the errors on the rates used to estimate time intervals between younger disturbance events (Table 4; Table DR2, see footnote 1). Disturbance event 17 is so much older than disturbance event 16 that its age is best estimated only with ^{14}C ages.

Through addition of our estimates of the number of years between disturbance events to the OxCal sequence analysis, we increase the precision (narrow the OxCal-derived age distribution ranges) of most of the ages for disturbance events 2–16 (Fig. 14). The most significant increases in precision are for disturbance events whose ages are closest in time (disturbance events 2 and 3, 8 and 9, and 11, 12, 13, and 14). Ages for disturbance events 5/6, 7, 15, and 16 are too widely separated in time from ages for adjacent disturbance events to be affected by the sequence analysis (age ranges are reduced by <20 yr).

HISTORY OF OUTLET ELEVATION FOR BRADLEY LAKE

The outlet elevation determines how easily the sea can enter the lake. A history of the elevation of Bradley Lake's outlet can be deduced from the relative sea-level curve of Witter et al. (2003) (Fig. 15) for the Sevenmile Creek estuary 14 km to the NNW (Fig. 1). We relate sea level to the elevation of the lake bottom by assuming that at the time China Creek was blocked by a dune, the lake floor probably stood 1–2 m above mean tide level (MTL) (Fig. 15); the incipient dune-dammed lake inundated a freshwater marsh that required an elevation more than a meter above mean tidal level.

Outlet elevation (that is, elevation relative to MTL) is the sum of the lake bottom elevation and the lake depth. Placing constraints on the lake depth through time places constraints on the outlet elevation through time. The buildup or erosion of the dune that blocks China Creek controls lake depth. Over time dunes accreted seaward of Bradley Lake (Fig. 2), resulting in stabilization of the oldest dune by vegetation, precluding further dune buildup. Increasingly younger foredunes seaward of the lake outlet (Fig. 2) indicate the ocean was closest to the lake just after it formed and the shoreline became increasingly more distant from the lake outlet as relative sea level rose. The oldest dune, which dams the lake, could build up only and thus deepen the lake early in the lake's history when the dune was active as a beach foredune. Erosion by tsunamis or storm surges could erode the lake outlet after it was stabilized by vegetation, thereby lowering lake depth; however, it is unlikely that the outlet would aggrade and the lake would deepen once the dune became stabilized by vegetation.

Lake lamination provides a clue to lake depth. Prior to 6000 yr B.P., most lake mud is faintly laminated to massive (Fig. 15B). Exceptions are the first two disturbance event sequences (events 17 and 16), which show finely laminated mud overlain by faintly laminated mud or massive mud. Sediment in Bradley Lake dating from ~6000 yr ago to present has well-preserved laminations. Preservation of laminations, which implies lack of bioturbation or wind turbation of the lake bottom, is typical of temperate-climate lakes at least 5 m deep (Larsen and MacDonald, 1993).

We infer from discontinuously preserved lake lamination in the first ~1300 yr that lake levels fluctuated during the early history of the lake (Fig. 15).The lake deepened rapidly, to at least 5 m, within a few hundreds of years of lake inception following disturbance event 17, as shown by finely laminated mud deposited after event 17. Then it fluctuated, up until sometime between disturbance events 15 and 16, between depths too shallow for laminae to be preserved to depths that favored preservation (Fig. 15). Because faintly laminated to massive mud dating from the past 6000 yr B.P. is uncommon, we infer that the lake has been deeper than 5 m for nearly all of that time (Fig. 15).

Buildup of seaward foredunes helped stabilize the lake outlet and protect it from all but the most extreme ocean levels. Protection of the lake outlet probably started ~1300 yr after lake inception, when lake lamination started to be preserved. If the lake outlet has remained stable since 6000 yr ago (1300 yr after lake inception) then the lake at that time reached a depth at least 15.5 m, which is the sum of the present lake depth (~9.5 m) plus the extent to which the lake has filled in with lacustrine sediment (~6 m) since that time. The lake could have been deeper because the outlet could have been eroded during disturbance events when ocean water entered the lake. Therefore, although lake depth may have rapidly decreased during some disturbance events, it never decreased to less than ~5 m.

Since 6000 yr ago, the lake outlet elevation has dropped relative to sea level because the bottom elevation has decreased as relative sea level rose, and the lake depth decreased as the lake bottom aggraded. If erosion was minimal, then from 6000–2500 yr B.P. the lake outlet elevation (relative to sea level) dropped from ~12.5 m to 6.5 m. In the last 2500 yr, lake outlet elevation dropped more slowly from 6.5 m to 5.5 m (Fig. 15).

DISCUSSION

Marine Incursions During Disturbance Events

Marine diatoms in disturbance event sediment demonstrate no fewer than 13 marine incursions into Bradley Lake in the past 7300 yr (Fig. 12; Tables 2 and 6). The first marine incursion, disturbance event 17, occurred when the lake formed ~7300 yr B.P. The first marine incursion is unique because there was no lake; instead, marine diatoms transported with sand were deposited on a freshwater marsh. In the absence of a lake, the disturbance event 17 sand is not overlain by massive organic-rich mud, a facies typical of subsequent marine incursions where suspended sediment settled out of a water column. None of the three succeeding disturbance events (16, 15, 14) left a record of fossil marine diatoms, although event 16 (6510–

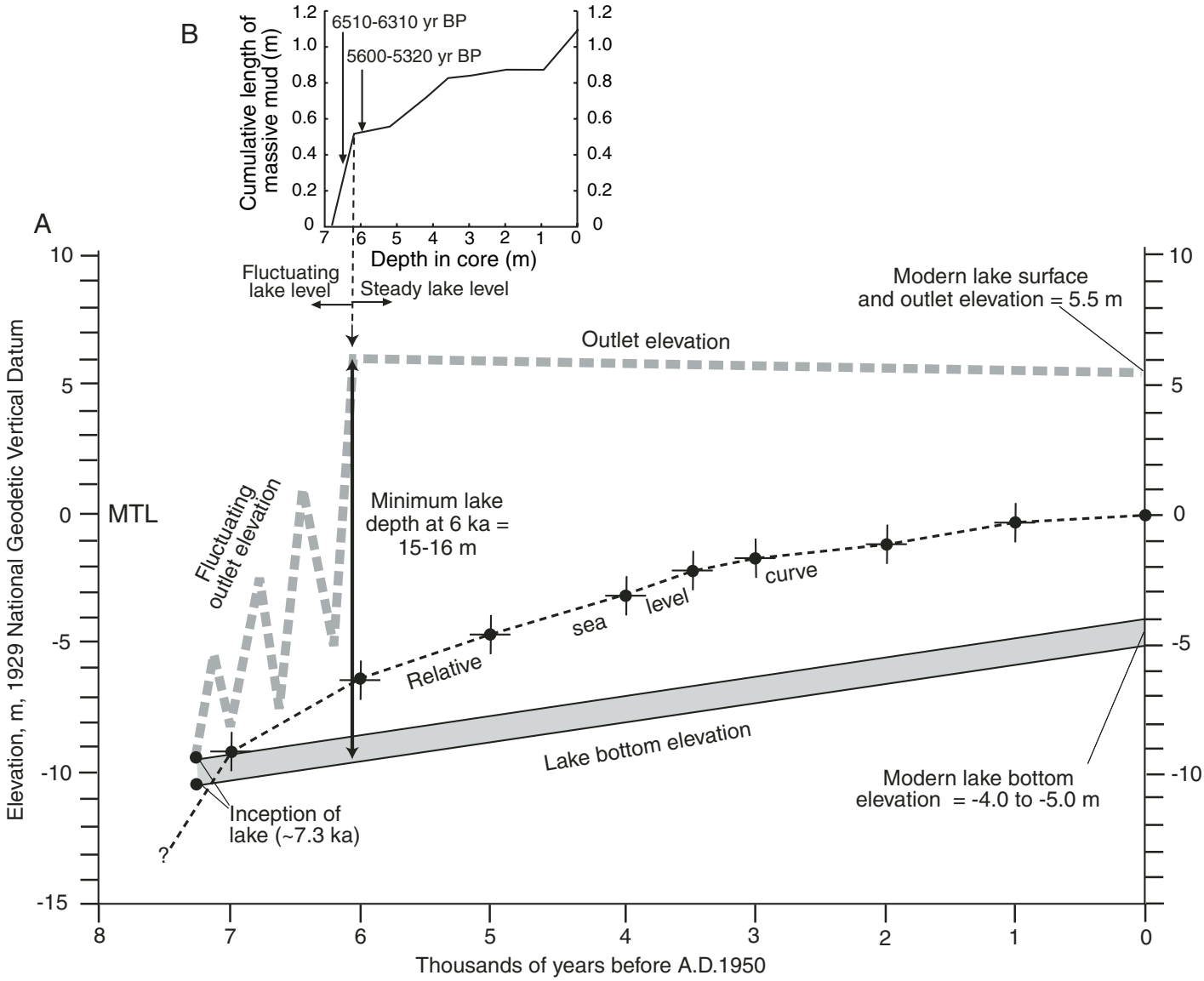

Figure 15. (A) Lake surface and outlet elevation relative to sea level (MTL, mean tide level). Relative sea-level curve (Witter et al., 2003) incorporates effects of tectonic uplift, which has been determined independently from marine terrace studies to be 0.2–0.5 mm/yr (McInelly and Kelsey, 1990) and eustatic sea-level rise. Lake surface and outlet elevation history assumes that the lake formed at 7.3 yr B.P. (Table 4) when the lake bottom was at, or no more than 1.0 m higher than, sea level. Lake bottom elevation relative to sea level is constrained by being equivalent to (or no more than 1 m higher than) relative sea level at 7.3 yr B.P. and –4.5 to –5.5 m at present (see further discussion in text). (B) Distribution of massive mud in the 6.8 m lacustrine sediment column, based on detailed inventory in cores D and BB. In the lower 0.5 m, almost all the sediment is massive; in the upper 6.3 m of the sediment column, 90% of the sediment is laminated. The two calibrated age ranges for disturbance events 16 and 15 (6510–6310 yr B.P. and 5600–5320 yr B.P. respectively) bracket the time, ~6000 yr B.P., at which lake level ceased fluctuating and sediment laminae were consistently preserved.

6310 yr B.P.) caused a bloom of the brackish diatom *T. bramaputrae* (Fig. 12). All subsequent disturbance events (starting with event 13 at 4630–4460 yr B.P.) except one (disturbance event 3, 1130–980 yr B.P.) were accompanied by marine incursions (Table 2).

The second facies association of each of the 12 marine incursions since 4600 yr B.P., although different in detail, is similar in several important characteristics. All have massive organic-rich mud overlain by finely laminated mud, and all have fossil Holocene marine diatoms in the disturbance event sediment. The 12 marine incursions have differing amounts of sand associated with them, but 6 of the 12 incursions deposited sand along the entire length of the lake (Fig. 16; Table 2). Seven of 12 of the marine incursions were followed by a bloom of brackish diatoms (Fig. 12, Table 2). Blooms of brackish diatoms possibly occurred in the other five marine incursions but more detailed diatom analyses are needed to document this inference.

The ocean water that entered Bradley Lake during disturbance events settled to the lake bottom. In the resulting meromictic lake, the upper water mass did not mix with denser, more saline bottom water (e.g., Wetzel, 2001). The

resultant chemocline (salinity gradient boundary zone at the top of the saline bottom layer) allowed diffusion of dissolved solids to shallow depths when the lake was isothermal in winter months (Fig. 5). Diatom assemblages show that the lake became slightly brackish after disturbance events, although not to the extent that freshwater diatom species were eliminated. A slightly brackish lake (up to 4 g/L salinity) was probably produced by diffusion across the chemocline; diffusion persisted for years to decades until saline bottom water was depleted. Today, ~300 yr since the last lake-wide disturbance, the bottom water is fresh.

During a marine incursion into the lake, ocean water surged up the beach and continued into the outlet channel into the lake. The surge entrained sand picked up from nearshore, beach, and dune environments and deposited the sand on the lake bottom. Coarsening and increasing sand thickness in a seaward direction and the presence of Holocene marine diatoms are consistent with the sand being transported into the lake from the ocean (Figs. 9B, 10, and 12). On the basis of multiple fining-upward sand beds in the sandy sequences (Fig. 11; Tables 2 and 3), we infer that marine incursions entail multiple surges of ocean water into the lake.

In the first few hours to a day following all marine incursions except the initial one (17), an organic-debris layer composed of mud encrusted twigs, small branches, and leaves settled to the bottom to produce the debris-rich mud facies. In subsequent days, suspended sediment settled to the lake bottom as a massive organic-rich mud (Fig. 9A). The debris-rich mud and the massive organic-rich mud are suspension deposits generated by sublacustrine slumps and by erosion and resuspension of sediment at the sediment-water interface as the surge of marine water traveled along the lake floor.

The bloom of brackish diatoms following marine incursion (Figs. 12 and 13) and the finely laminated mud facies overlying the massive organic-rich mud (Figs. 6, 7, and 8) indicate that marine incursions instigate brackish lake conditions that suppress lake productivity and decrease rates of organic sedimentation. The duration of suppressed lake productivity is on the order of 5 yr to several decades, based on counts of light-dark couplets of finely laminated mud above the massive organic-rich mud (Table 2).

TABLE 6. FREQUENCY DATA FOR CASCADIA SUBDUCTION ZONE EARTHQUAKES, USING TIDAL MARSH PALEOSEISMIC RECORDS AT LEAST 3500 YEARS IN DURATION

Data source	Duration of stratigraphic record (yr)	Number of inferred subduction zone earthquake events	Average interval between events (yr)
Atwater and Hemphill-Haley (1997)	3500	7	500–540†
Witter et al. (2003)	6600	12	570–590
Kelsey et al. (2002)	5500	11	480–535

Note: Process recording the earthquakes is coseismic subsidence that causes an abrupt rise in sea level resulting in tidal mud burying marsh soil.
†The longest interval is between 700 and 1300 yr; the shortest interval is no longer than 450 yr.

Evaluation of Tsunamis as Mechanisms of Marine Incursion

Hypothetically, several mechanisms could raise marine water into Bradley Lake. We will show that the most likely of these are tsunamis generated nearby, by seismically induced seafloor displacement above the Cascadia subduction zone. However, we also consider the possibility of incursions from far-traveled tsunamis generated elsewhere on the Pacific Rim. In addition, we consider the possibility that climatically induced extreme ocean levels, further elevated by wave runup, spilled marine water into the lake.

Viable mechanisms of marine incursion must satisfy height and duration constraints. For the past 6000 yr, the ocean height that would allow spillover across into the lake must have been at least 5.5–8 m above mean sea level (Fig. 15). The minimum required duration of marine spillover to produce the characteristic disturbance event features is not as well constrained as the height, but a sustained flow of ocean water is required to transport nearshore and beach sand into the lake and to erode the lake floor.

The best constraint on the duration of marine incursion is the triggering, in at least seven instances, of an episode of brackish lake conditions after the incursion. The volume of ocean water that must have entered the lake in order to increase salinity to 2–4 g/L can be estimated by assuming a meromictic lake with slow diffusion of basal saline water. The duration of ocean inflow that would have set up the brackish lake conditions must have been at least 10 min and probably longer (see calculations in Appendix).

A local tsunami generated at the Cascadia subduction zone satisfies the requirement of sustained, elevated ocean discharge into Bradley Lake. A subduction zone earthquake, because it warps the seafloor above the zone of rupture over a width of many tens of kilometers, generates a tsunami tens of kilometers in wavelength. Such a wavelength allows for a longer duration marine incursion than wind-generated waves with wavelengths on the order of meters. Local tsunamis typically runup onto beaches at least 5 m and in most cases more than 6 m above mean tide level. Local tsunamis can attain runup elevations of 10–15 m. Local tsunamis occur in several pulses with each pulse, or surge, cresting at peak elevation for several to tens of minutes, long enough to entrain, transport, and deposit large quantities of marine water and sand in Bradley Lake. For instance, tide gage records reconstructed from eyewitness accounts on Kodiak Island in the 8 h following the moment magnitude M_w 9.2 1964 Prince William Sound (Alaska) earthquake indicate that local-tsunami-induced extreme ocean levels 5–8 m above mean lower low water persisted for at least 300 min, cumulatively spanning at least four separate tsunami waves (Wilson and Tørum, 1968). Similarly, at Seward, Alaska, extreme ocean levels >5 m persisted for at least 60 min (Wilson and Tørum, 1968). At other coastal sites in Alaska where duration data are unavailable, maximum tsunami runup for the 1964 earthquake often was ≥9 m (10 observations) (National Geophysical Data Center, 1998). Local tsunami runup heights in Chile immediately following the 1960 M_w 9.5 Chile earthquake exceeded 9 m at several sites (7 observations), and at two of these coastal sites runup reached 25 m elevation (National Geophysical Data Center, 1998). Records for the only tide gage in Chile located near (north of) the 22 May 1960 plate-boundary rupture (Talcahuano) show that the first four tsunami waves had periods of 50–80 min, peak heights up to 5.5 m, and inundation durations at the peak heights that spanned 10–20 min (Sievers et el., 1963). Observations of local tsunamis from great (>M_w 8) subduction zone earthquakes show that local tsunamis can supply the sustained, elevated ocean head necessary to carry marine water and marine sand into elevated coastal lakes.

Local tsunamis can account for the inferred frequency of the marine incursions. Cascadia subduction zone earthquakes, which generate local Cascadia subduction zone tsunamis, have an average return period (Table 6) consistent with the frequency of marine incursions (Fig. 16).

Far-traveled tsunamis can, at best, marginally satisfy the 5.5–8 m height requirement and only for the greatest earthquakes. The 1964 M_w 9.2 Prince William Sound, Alaska, earthquake generated tsunami runups on the west coast of Canada and the United States of less than 3.5 m

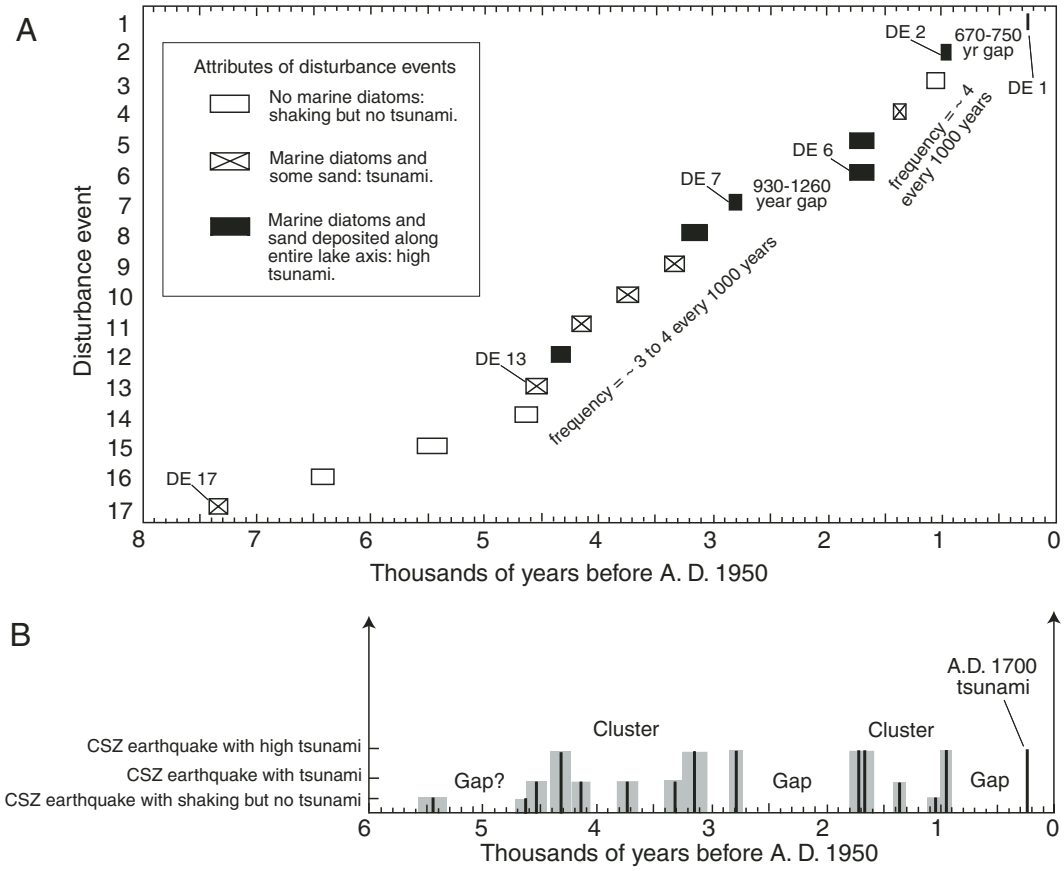

Figure 16. (A) Frequency of disturbance events since the lake formed ~7300 yr B.P. (DE—Disturbance event). Age ranges for disturbance events are OxCal-derived age ranges from Table 4. (B) Inferred great earthquake history for the Cascadia subduction zone from Bradley Lake tsunami record. Width of shaded bar denotes age uncertainty of tsunami, thinner solid bar denotes median of age range. The two tsunamis at 1700 yr B.P. (years before A.D. 1950) are at least 22 yr apart.

(17 observations), except for a 5.1 m runup at Crescent City in northern California (National Geophysical Data Center, 1998; Witter et al., 2001). The maximum runup in Japan from the 1960 Chile earthquake was 6 m at the upper end of a bay that amplified the tsunami height, and most observations of runup in Japan were 4 m or less (Committee for Field Investigation of the Chilean Tsunami of 1960, 1961; Satake et al., 2003). The 23 and 24 December 1854 pair of M 8.3–8.4 earthquakes on the Nankai trough in Japan (Ando, 1975) each generated tsunamis recorded on the U.S. west coast (at tides gauges in Astoria, Oregon, and San Francisco and San Diego, California) of <0.1 m amplitude (Lander et al., 1993). These same earthquakes generated tsunami waves that reached runup heights of 5–20 m in Japan (Watanabe, 1998). Far-traveled tsunamis from the 1946 Aleutian earthquake and the 1960 Chile earthquake generated up to 16.4 m waves (Aleutian tsunami) and up to 10.7 m waves (Chilean tsunami) in Hawaii but had minor effects (most wave heights <1 m; maximum of 1.9 m) on the west coast of the United States because of the long diagonal approach of tsunami waves from Alaskan or South American subduction zones (Shepard, 1963; Lander et al., 1993).

Climatically induced extreme ocean level is not a viable mechanism for marine incursions into Bradley Lake. In coastal Oregon, extreme ocean levels of 5.5–8 m can be generated by climatic mechanisms, at recurrence intervals of tens of years, only if wave runup is superposed on extreme ocean level caused by astronomic tides, storm surge, and El Niño–Southern Oscillation phenomena (Witter et al., 2001). Without wave runup, extreme ocean levels do not surpass 3 m, even at recurrence intervals of hundreds of years. Wave runup is generated by ocean waves, and periods of oceans waves with maximum amplitude at the latitude of central Oregon are on the order of 9–17 s (National Data Buoy Center, 2002). Marine incursion to Bradley Lake requires that extreme ocean levels travel the 300–500 m distance from the beach to the lake outlet (Fig. 2) and that a hydraulic head of greater than 5 m above mean sea level be maintained long enough to sustain flow from ocean to lake. Transient, seconds-long instances of wave runup cannot provide the sustained, greater-than-5.5-m ocean levels required to produce widespread lake bottom erosion and sand deposition and to trigger brackish lake conditions.

In the special case of disturbance event 17, in which marine water inundated a freshwater marsh and not a preexisting lake, the mechanism of deposition of marine-diatom–laden sand is either local tsunami or climatically induced extreme ocean levels. Because deposition and erosion associated with disturbance event 17 is extensive (the sand extends the full length of the lake, contains rip-up clasts, and the basal sand contact is eroded, Table 2), we infer that a local tsunami is the mechanism of marine incursion.

In conclusion, the 12 disturbance events that involve marine incursion since 4600 yr B.P. occurred as a consequence of local tsunamis produced by earthquakes on the Cascadia subduction zone. Although the tsunamis recorded in Bradley Lake are entirely or mostly triggered by coseismic, tectonically driven seafloor displacement, it is possible that some tsunamis in Bradley Lake are in part generated by earthquake-triggered submarine landslides near Bradley Lake that failed during or immediately following seismic shaking (e.g., Synolakis et al., 2002).

The massive organic-rich mud of disturbance events that are not accompanied by marine incursion (3, 14, 15, and 16) may be the product of seismically triggered sublacustrine slope failures. Deposition of massive organic-rich mud

over the entire lake bottom without an accompanying marine incursion requires resuspension of lake sediment in the water column by a process that acted over the entire lake. Multiple failures of the steep flanks of the lake could stir up the lake bottom and cause deposition of massive organic-rich mud. In the case of disturbance event 3, whose beds lack Holocene marine diatoms, collapse of a submerged dune probably contributed sand to the lake floor (Table 2). The slope failures probably were seismically triggered because a high-magnitude, short-duration impulsive trigger such as an earthquake is necessary to trigger multiple slope failures.

History and Frequency of Tsunamis

Bradley Lake was a less effective tsunami recorder during its first 2600 yr (Fig. 16), probably because the outlet was too high (Fig. 15). Bradley Lake became a good recorder of tsunamis at ~4600 cal yr B.P. when the lake outlet elevation dropped to ~9–10 m (Fig. 15).

The highest tsunamis are those that eroded the lake bottom, deposited the thickest and most extensive sand beds, and imported the greatest number of marine diatoms into the lake (Fig. 16; Table 2). Judged by their record, the highest tsunamis are disturbance events 2, 5, 6, 7, 8, and 12 (Fig. 16).

Tsunamis in Bradley Lake are clustered in time. Between 4600 and 2800 cal yr B.P., tsunamis occurred at an average frequency of ~3–4 every 1000 yr (Fig. 16). Then, starting ~2800 cal yr B.P., there was a 930–1260 yr interval with no tsunamis. That gap was followed by a ~1000 yr period with 4 tsunamis. In the last millennium, a 670–750 yr gap preceded the A.D. 1700 tsunami (Fig. 16).

The highest tsunamis tend to be at the beginning and end of clusters. For instance, the tsunamis of events 7 and 6 bracket the 930–1260 yr gap; similarly, the high event 2 tsunami and the A.D. 1700 tsunami bracket the 670–750 yr gap (Fig. 16). Thatcher (1990) proposes that during seismic cycles in the circum-Pacific region, the greatest earthquakes tend to terminate a cycle followed by seismic quiescence at the start of the next cycle. Such a pattern is consistent with the Bradley Lake tsunami record where two of the highest tsunamis (7, 2) immediately precede a gap in the tsunami record (Fig. 16B). The pattern suggests that the M_w 9 A.D. 1700 subduction zone earthquake (Satake et al., 2003) might have initiated a new cluster of earthquakes in the present seismic cycle (Fig. 16B).

Evidence that the lake is perhaps a less effective recorder now than in the past few millennia is the lake's minimal stratigraphic record of the A.D. 1700 Cascadia tsunami (Tables 2 and 3). This tsunami, although generated by a ~M_w 9 earthquake (Satake et al., 2003), delivered negligible sand to Bradley Lake, did not cause extensive erosion of the lake bottom, and did not trigger a bloom of brackish diatoms. Although the outlet elevation is the lowest since the lake ceased fluctuating 6000 yr ago (Fig. 15), the outlet is also further inland than at any time in the history of the lake. Increasing travel distance for a tsunami to the lake outlet more than offsets decreasing outlet height (Hutchinson et al., 1997).

The average of the recurrence intervals of Bradley Lake tsunami incursion is shorter than the average of the recurrence intervals inferred for great earthquakes elsewhere along the Cascadia subduction zone. Both at Bradley Lake (Fig. 16) and elsewhere [for example, Sixes River estuary, Oregon (Kelsey et al., 2002) and Willapa Bay, Washington (Atwater and Hemphill-Haley, 1997)], the individual recurrence intervals vary from a few decades to 1200 yr. The average recurrence interval for incursion to Bradley Lake is ~380–400 yr, calculated as the average length of 11 intervals in a time period from 4460–4630 yr B.P. to 250 yr B.P. The average is shorter than the 480–590 yr average earthquake return period at individual Cascadia tidal marsh sites, including two sites, Sixes River and Coquille River estuary, that are within 28 km of Bradley Lake (Atwater and Hemphill-Haley, 1997; Kelsey et al., 2002; Witter et al., 2003) (Table 6).

The high frequency of tsunamis at Bradley Lake supports the idea that rupture lengths vary among great earthquakes on the Cascadia plate boundary (Kelsey et al., 2002; Witter at al. 2003). Bradley Lake can record tsunamis from rupture of the entire length of the plate boundary, rupture of a segment that underlies Bradley Lake, and rupture of an adjoining segment to the north or south. In contrast, a coastal marsh site recording coseismic subsidence will only record subduction zone earthquakes caused by local plate-boundary rupture. Tsunamis from rupture of an adjoining segment of the plate boundary did not deposit sand at either the Sixes River or Coquille River tidal marsh sites because sand deposits beneath these marshes only occur directly overlying buried marsh soils that subsided during plate-boundary earthquakes.

Some of the tsunamis that entered Bradley owe their origin to rupture on adjacent segments. For instance, the tsunamis that caused disturbance events 5 and 6 probably were generated by two plate-boundary earthquakes only a few decades apart (Table 4). It is likely that only one of these tsunamis was generated by earthquake 3 at the Coquille River (Witter et al., 2003), which overlaps in time with disturbance events 5 and 6. The other tsunami probably was generated further north along the plate boundary, where earthquake S at Willapa Bay overlaps in time with disturbance events 5 and 6 (Atwater and Hemphill-Haley, 1997).

Earthquakes on upper plate faults that occur independently of, and are not triggered by, Cascadia plate-boundary earthquakes may produce tsunamis that could leave a record in Bradley Lake; however, such a tsunami source is undocumented. Coastal paleoseismological studies in southern Oregon (Kelsey et al., 2002; Witter et al., 2003) could not document that such earthquakes occur because tsunami sand beneath coastal marshes only is found in association with regionally extensive buried soils that subsided during regionally extensive plate-boundary ruptures. Atwater and Hemphill-Haley (1997) argue a similar case against upper-plate faults as causes for coseismic subsidence in southwestern Washington. During the 1964 Alaska plate-boundary earthquake, an associated upper-plate fault did rupture, and this upper-plate earthquake contributed to the height of the 1964 tsunami. However, the combined upper-plate earthquake and plate-boundary earthquake cannot be distinguished as separate earthquakes in the geologic record (Plafker, 1969).

CONCLUSIONS

For the past 7300 yr, since it was formed by dune damming of China Creek following disturbance event 17, Bradley Lake has been a freshwater lake ~500 m or less inland of the coast. Sixteen times since lake inception, the annual cycle of sedimentation in Bradley Lake was disturbed by events that resuspended sediment from the bottom and the sideslopes of the lake. In the 12 most extreme cases, the disturbance involved a surge of marine water that entered the lake and settled on the lake bottom, introducing marine diatoms and leaving a deposit of organic debris and sand that was subsequently blanketed by massive organic-rich mud.

For the 12 disturbance events, a tsunami generated by plate-boundary rupture along the Cascadia subduction zone is the only process that can collectively satisfy the magnitude and duration constraints demanded by the lithostratigraphic and biostratigraphic evidence from Bradley Lake. Seismic shaking also is the most likely trigger for the four events that did not introduce marine diatoms into the lake.

Over the 4600 yr period when Bradley Lake was the optimum tsunami recorder, tsunamis entered Bradley Lake an average of every 380–400 yr, whereas the portion of the Cascadia plate boundary that underlies Bradley Lake rup-

tured in a great earthquake less frequently (only once every 480–590 yr). Therefore, the Bradley Lake record includes earthquakes caused by rupture along the entire length of the Cascadia plate boundary as well as earthquakes caused by rupture of shorter segments of the boundary, supporting contentions (Kelsey et al., 2002; Witter et al., 2003) that the entire length of the plate boundary does not rupture in every earthquake. The tsunami record from Bradley Lake indicates that at times, most recently ~1700 yr B.P., overlapping or adjoining segments of the plate boundary rupture within decades of each other.

Local tsunamis from Cascadia plate-boundary earthquakes recur in clusters (every ~250–400 yr) followed by gaps of 700–1300 yr. The highest tsunamis apparently occur at the beginning and end of clusters. The most recent earthquake and tsunami (A.D. 1700) might be at the beginning of a new cluster of tsunamis accompanying great earthquakes.

APPENDIX: CALCULATION OF DURATION OF MARINE SPILLOVER

The calculation of the duration of marine spillover into Bradley Lake assumes that a brackish diatom bloom is triggered by an increase in salinity of the lake up to the limit of brackish diatom tolerance (~2‰–4‰). The elapsed time of a marine incursion into the lake must be long enough to account for outflow of brackish water (up to 4‰) from the lake for at least one to more than 10 yr after disturbance. Given the 4900×10^3 m^3 annual lake discharge (Table 1), the volume of ocean water entering the lake during a disturbance needs to be 280×10^3 to 560×10^4 m^3, if ocean water (35‰) is diluted by factors of 17.5 (2‰) to 8.75 (4‰) before being discharged from the lake over time periods of 1–10 yr after disturbance.

Using hydraulic parameters that minimize duration of ocean inflow [maximum tsunami velocity = 20 m/s (Toshihiko et al., 1995), maximum outlet cross sectional area = 20 m^2, minimum length of time that the lake was brackish = 1 yr], ocean water must have flowed into the lake for at least 10–20 min to import enough ocean water to accommodate 1 yr of diluted (2‰–4‰) discharge. Other durations using more physically reasonable estimates of tsunami velocity (5–15 m/s), outlet channel cross sectional area (8–12 m^2), and durations of brackish water discharge (5–10 yr) give durations of marine incursion from 2 to 15 h. Therefore, extreme ocean levels of 5–8 m above mean sea level must have durations of 10–900 min. The total duration is probably the sum of several instances of spillover.

ACKNOWLEDGMENTS

The National Science Foundation (NSF) (EAR-9405263) and the National Earthquake Hazards Reduction Program of the U.S. Geological Survey provided financial support. Cathy Whitlock lent piston-coring equipment and a coring platform, and Ian Hutchinson gave advice on coring. Richard Marzolf lent us an echo sounder. Tom Stafford prepared targets for initial ^{14}C ages. Roger Lewis prepared and analyzed sediment and numerous diatom samples. Dustin Dawson, Laurie Griggs, Tom Halferty, Jeff Ollerhead, and Mark Verona helped in the field. Cores were stored at the NSF-funded core storage facility at Oregon State University, coordinated by Bobbi Conard. ^{14}C analyses provided by the NSF Accelerator Facility at the University of Arizona. Carrie Garrison-Laney and Lee-Ann Bradley helped with graphics. Ian Shennan, Mark Petersen, David Perkins, Jody Bourgeois, and Hans Nelson provided helpful discussion. Reviews by Brian Atwater, John Clague, Ian Hutchinson, John Major, Brian Sherrod, and Bob Yeats substantially improved the paper.

REFERENCES CITED

Abramson, H., 1998, Evidence for tsunamis and earthquakes during the last 3500 years from Lagoon Creek, a coastal freshwater marsh, northern California [M.S. thesis]: Arcata, Humboldt State University, 76 p.

Adams, J., 1990, Paleoseismicity of the Cascadia subduction zone, evidence from turbidites off the Oregon-Washington margin: Tectonics, v. 9, p. 569–583.

Anderson, R.Y., 1996, Seasonal sedimentation: A framework for reconstructing climatic and environmental change, *in* Kemp, A.E.S., ed., Palaeoclimatology and palaeooceanography from laminated sediments: The Geological Society [London] Special Publication 116, p. 1–15.

Ando, M., 1975, Source mechanisms and tectonic significance of historical earthquakes along the Nankai trough, Japan: Tectonophysics, v. 27, p. 119–140.

Aspila, K.I., Agemian, H., and Chau, A.S.Y., 1976, A semi-automated method for the determination of inorganic, organic and total phosphate in sediments: Analyst, v. 101, p. 187–197.

Atwater, B.F., 1987, Evidence for great Holocene earthquakes along the outer coast of Washington state: Science, v. 236, p. 942–944.

Atwater, B.F., and Hemphill-Haley, E., 1997, Recurrence intervals for great earthquakes of the past 3500 years at northeastern Willapa Bay, Washington: U.S. Geological Survey Professional Paper 1576, 108 p.

Birks, H.J.B., 1981, Late Wisconsin vegetational and climatic history at Kylen Lake, north-eastern Minnesota: Quaternary Research, v. 16, p. 322–355.

Bondevik, S., Svendsen, J.I., and Mangerud, J., 1997, Tsunami sedimentary facies deposited by the Storegga tsunami in shallow marine basins and coastal lakes, western Norway: Sedimentology, v. 44, p. 1115–1131.

Boulter, M.C., 1994, An approach to a standard terminology for palynodebris, *in* Traverse, A., ed., Sedimentation of organic particles: Cambridge, UK, Cambridge University Press, p. 199–216.

Bradbury, J.P., and Dean, W.E., 1993, Elk Lake, Minnesota: Evidence for rapid climate change in the north-central United States: Geological Society of America Special Paper 276, 336 p.

Bronk Ramsey, C., 1995, Radiocarbon calibration and analysis of stratigraphy: The OxCal program: Radiocarbon, v. 37, p. 425–430.

Bronk Ramsey, C., 2001, Development of the radiocarbon program OxCal: Radiocarbon, v. 43, p. 355–363.

Carpelan, L.H., 1978, Revision of Kolbe's System der Halobien based on diatoms of California lagoons: Oikos, v. 31, p. 112–122.

Clague, J.J., 1996, Paleoseismology and seismic hazards: Geological Survey of Canada Bulletin 494, 88 p.

Clague, J.J., and Bobrowsky, P.T., 1994, Evidence for a large earthquake and tsunami 100–400 years ago on western Vancouver Island, British Columbia: Quaternary Research, v. 41, p. 176–184.

Clague, J.J., Bobrowsky, P.T., and Hutchinson, I., 2000, A review of geological records of large tsunamis at Vancouver Island, British Columbia, and implications for hazard: Quaternary Science Reviews, v. 19, p. 849–863.

Committee for Field Investigation of the Chilean Tsunami of 1960, 1961, Report on the Chilean tsunami of May 24, 1960, as observed along the coast of Japan: Tokyo, Maruzen Co., Ltd., 397 p.

Cumming, B.F., and Smol, J.P., 1993, Development of diatom-based salinity models for paleoclimatic research from lakes in British Columbia (Canada): Hydrobiologia, v. 269/270, p. 179–196.

Darienzo, M.E., and Peterson, C.D., 1990, Episodic tectonic subsidence of late Holocene salt marshes, northern Oregon central Cascadia margin: Tectonics, v. 9, p. 1–22.

Dean, J.M., Kemp, A.E.S., Bull, D., Pike, J., Patterson, G., and Zolitschka, B., 1999, Taking varves to bits: Scanning electron microscopy in the study of laminated sediments and varves: Journal of Paleolimnology, v. 22, p. 121–136.

Dunne, T., and Leopold, L.B., 1978, Water in Environmental Planning: San Francisco, W.H. Freeman and Co., 818 p.

Foged, N., 1981, Diatoms in Alaska: Bibliotheca Phycologia, v. 53, 316 p.

Fritz, S.C., Juggins, S., and Battarbee, R.W., 1993, Diatom assemblages and ionic characterization of lakes of the northern Great Plains, North America: A tool for reconstructing past salinity and climate fluctuations: Canadian Journal of Fisheries and Aquatic Sciences, v. 50, p. 1844–1856.

Garrison-Laney, C., 1998, Diatom evidence for tsunami inundation from Lagoon Creek, a coastal freshwater pond, Del Norte County, California [M.S. thesis]: Arcata, Humboldt State University, 97 p.

Garwood, A.N., ed., 1996, Weather America—The latest detailed climatological data for over 4000 places: Milpitas, California, Toucan Valley Publications, 1412 p.

Goldfinger, C., Nelson, C.H., and Johnson, J.E., 2003, Holocene earthquake records from the Cascadia subduction zone and northern San Andreas fault based on precise dating of offshore turbidites: Annual Review of Earth and Planetary Sciences, v. 31, p. 555–577.

Hedges, R.E.M., 1991, AMS dating: Present status and potential applications, *in* Lowe, J.J., ed., Radiocarbon dating: Recent applications and future potential: Cambridge, UK, Quaternary Research Association, p. 5–9.

Hemphill-Haley, E., 1996, Diatoms as an aid in identifying late-Holocene tsunami deposits: The Holocene, v. 6, p. 439–448.

Hemphill-Haley, E., and Lewis, R.C., 2003, Diatom data from Bradley Lake, Oregon: Downcore analyses, U.S. Geological Survey Open-File Report 03-190, 129 p.

Hughen, K., 1996, The potential for palaeoclimatic records from varved Arctic lake sediments: Baffin Island, eastern Canadian Arctic, *in* Kemp, A.E.S., ed., Palaeoclimatology and palaeooceanography from laminated sediments: The Geological Society [London] Special Publication 116, p. 57–71.

Hutchinson, I., Clague, J.J., and Mathewes, R.W., 1997, Reconstructing the tsumani record on an emerging coast: A case study of Kanim Lake, Vancouver Island, British Columbia, Canada: Journal of Coastal Research, v. 13, p. 545–553.

Hutchinson, I., Guilbault, J.-P., Clague, J.J., and Bobrowsky, P.T., 2000, Tsunamis and tectonic deformation at the northern Cascadia margin: A 3000 year record from Deserted Lake, Vancouver Island, British Columbia, Canada: The Holocene, v. 10, p. 429–439.

Jacoby, G.C., Bunker, D.E., and Benson, B.E., 1997, Tree-ring evidence for an A.D. 1700 Cascadia earthquake in Washington and northern Oregon: Geology, v. 25, p. 999–1002.

John, J., 1983, Observations on *Thalassiosira lacustris* (Grunow) Hasle populations from western Australia: Nova Hedwigia, v. 38, p. 323–337.

Kelsey, H.M., Witter, R.C., and Hemphill-Haley, E., 1998, Response of a small Oregon estuary to coseismic subsidence and postseismic uplift in the past 300 years: Geology, v. 26, p. 231–234.

Kelsey, H.M., Witter, R.C., and Hemphill-Haley, E., 2002, Plate-boundary earthquakes and tsunamis of the past 5500 yr, Sixes River estuary, southern Oregon: Geological Society of America Bulletin, v. 114, p. 298–314.

Lander, J.F., Lockridge, P.A., and Kozuch, M.J., 1993, Tsunamis affecting the west coast of the United States, 1806–1992, National Oceanic and Atmospheric Administration Geophysical Data Center Document 29, 242 p.

Larsen, C.P.S., and MacDonald, G.M., 1993, Lake morphometry, sediment mixing and the selection of sites for fine resolution palaeoecologic studies: Quaternary Science Reviews, v. 12, p. 781–792.

Larsen, C.P., Pienitz, R., Smol, J.P., Moser, K.A., Cumming, B.F., Blais, J.M., MacDonald, G.M., and Hall, R.I., 1998, Relations between lake morphometry and the presence of laminated lake sediments: A re-examination of Larsen and MacDonald (1993): Quaternary Science Reviews, v. 17, p. 711–717.

McInelly, G.W., and Kelsey, H.M., 1990, Late Quaternary tectonic deformation in the Cape Arago–Bandon region of coastal Oregon as deduced from wave-cut platforms: Journal of Geophysical Research, v. 95, p. 6699–6713.

National Data Buoy Center, 2002, Station 46050, Yaquina Bay, http://seaboard.ndbc.noaa.gov/.

National Geophysical Data Center, 1998, Worldwide tsunami database, natural hazards data, http://www.ngdc.noaa.gov/seg/hazard/.

Nelson, A.R., Jennings, A.E., and Kashima, K., 1996, An earthquake history derived from stratigraphic and microfossil evidence of relative sea level change at Coos Bay, southern coastal Oregon: Geological Society of America Bulletin, v. 108, p. 141–154.

Oldfield, F., 1977, Lakes and their drainage basins as units of sediment-based ecological study: Progress in Physical Geography, v. 1, p. 460–504.

Ojala, A.E.K., Saarinen, T., and Salonen, V.-P., 2000, Preconditions for the formation of annually laminated lake sediments in southern and central Finland: Boreal Environmental Research, v. 5, p. 243–255.

O'Sullivan, P.E., 1983, Annually laminated lake sediments and the study of Quaternary environmental changes—A review: Quaternary Science Reviews, v. 1, p. 245–311.

Page, M.J., Trustrum, N.A., and DeRose, R.C., 1994, A high resolution record of storm-induced erosion from lake sediments, New Zealand: Journal of Paleolimnology, v. 11, p. 333–348.

Peglar, S.M., Fritz, S.C., Alapieti, T., Saarnisto, M., and Birks, J.B., 1984, Composition and formation of laminated sediments in Diss Mere, Norfolk, England: Boreas, v. 13, p. 13–28.

Plafker, G., 1969, Tectonics of the March 27, 1964 Alaska earthquake: U.S. Geological Survey Professional Paper 543-I, 74 p.

Satake, K., Shimazaki, K., Tsuji, Y., and Ueda, K., 1996, Time and size of a giant earthquake in Cascadia inferred from Japanese tsunami records of January 1700: Nature, v. 379, p. 246–249.

Satake, K., Wang, K., and Atwater, B.F., 2003, Fault slip and seismic moment of the 1700 Cascadia earthquake inferred from Japanese tsunami descriptions: Journal of Geophysical Research, v. 108.

Shepard, F.P., 1963, Submarine Geology, 2nd Edition: New York, Harper and Row, 557 p.

Sievers H.A., Villegas, G., and Barros G., 1963, The seismic sea wave of 22 May 1960 along the Chilean coast: Bulletin of the Seismological Society of America, v. 53, p. 1125–1190.

Simola, H.K.L., Coard, M.A., and O'Sullivan, P.E., 1981, Annual laminations in the sediments of Loe Pool, Cornwall: Nature, v. 290, p. 238–241.

Smith, D.G., 1987, A mini-vibracoring system: Journal of Sedimentary Petrology, v. 57, p. 757–758.

Stanley, D.J., and Warne, A.G., 1994, Worldwide initiation of Holocene marine deltas by deceleration of sea level rise: Science, v. 265, p. 228–231.

Stuiver, M., Reimer, P.J., Bard, E., Beck, J.W., Burr, G.S., Hughen, K.A., Kromer, B., McCormac, G., and Plicht, Jv.D., and Spurk, M., 1998, INTCAL98 radiocarbon age calibration, 24,000–0 cal B.P.: Radiocarbon, v. 40, p. 1041–1084.

Synolakis, C.E., Bardet, J.-P., Borrero, J.C., Davies, H.L., Okal, E.A., Silver, E.A., Sweet, S., and Tappin, D.R., 2002, The slump origin of the 1998 Papua New Guinea tsunami: Proceedings of the Royal Society of London, Series A, v. 458, p. 763–789.

Taylor, R.E., Stuiver, M., and Reimer, P.J., 1996, Development and extension of the calibration of the radiocarbon time scale: Archaeological applications: Quaternary Science Reviews, v. 15, p. 655–668.

Thatcher, W., 1990, Order and diversity in the modes of circum-Pacific earthquake recurrence: Journal of Geophysical Research, v. 95, p. 2609–2624.

Thornthwaite, C.W., and Mather, J.R., 1955, The water balance: Centerton, New Jersey, Laboratory of Climatology Publication No. 8.

Toshihiko, T., Tsutsumi, A., Kawamoto, E., Miyawaki, M., and Sato, H., 1995, Field survey report on tsunami disasters caused by the 1993 southwest Hokkaido earthquake: Pure and Applied Geophysics, v. 145, p. 665–691.

Watanabe, H., 1998, Comprehensive list of destructive tsunamis in Japan, 2nd edition: Tokyo, University of Tokyo Press, 238 p. (in Japanese).

Wells, R.E., Blakely, R.J., Sugiyama, Y., Scholl, D.W., and Dinterman, P.A., 2003, Basin-centered asperities in great subduction zone earthquakes: A link between slip, subsidence, and subduction erosion?: Journal of Geophysical Research, v. 108, no. B10, p. 2507.

Wetzel, R.G., 2001, Limnology, 3rd edition: Philadelphia, A.B. Saunders, 767 p.

Whiting, M.C., and Schrader, H., 1985, Late Miocene to early Pliocene marine diatom and silicoflagellate floras from the Oregon coast and continental shelf: Micropaleontology, v. 31, p. 249–270.

Wilson, B.W., and Tørum, A., 1968, The tsunami of the Alaskan earthquake, 1964: United States Army Corps of Engineers, Coastal Engineering Research Center, Engineering Evaluation Technical Memorandum 25, 401 p.

Wilson, S.E., Cumming, B.F., and Smol, J.P., 1996, Assessing the reliability of salinity inference models from diatom assemblages: An examination of a 219-lake data set from western North America: Canadian Journal of Fisheries and Aquatic Sciences, v. 53, p. 1580–1594.

Witter, R.C., Kelsey, H.M., and Hemphill-Haley, E., 2001, Pacific storms, El Nino and Tsunamis, Competing mechanisms for sand deposition in a coastal marsh, Euchre Creek, Oregon: Journal of Coastal Research, v. 17, p. 563–583.

Witter, R.C., Kelsey, H.M., and Hemphill-Haley, E., 2003, Great Cascadia earthquakes and tsunamis of the past 6700 years, Coquille River estuary, southern coastal Oregon: Geological Society of America Bulletin, v. 115, p. 1289–1306.

Wohlfarth, B., Skog, G., Possnert, G., and Holmquist, B., 1998, Pitfalls in the AMS radiocarbon-dating of terrestrial macrofossils: Journal of Quaternary Science, v. 13, p. 137–145.

Wright, H.E., 1967, A square-rod piston sampler for lake sediments: Journal of Sedimentary Petrology, v. 37, p. 975–976.

Yamaguchi, D.K., Atwater, B.F., Bunker, D.E., Benson, B.E., and Reid, M.S., 1997, Tree-ring dating the 1700 Cascadia earthquake: Nature, v. 389, p. 922–923.

Manuscript Received by the Society 21 July 2003
Revised Manuscript Received 18 October 2004
Manuscript Accepted 14 December 2004

Printed in the USA